*Mon. Not. R. astr. Soc.* (1972) **157**, 179–210.

# ON THE INTERPRETATION OF RADIO RECOMBINATION LINE OBSERVATIONS

*M. Brocklehurst and M. J. Seaton*

(Received 1971 December 1)


## SUMMARY

A substantial amount of data from atomic physics is required for the interpretation of radio recombination line observations. A critical review of the available data is presented, and it is concluded that possible errors in this data are no larger than the errors which typically occur in the observational results.

The equation of transfer for the line radiation is discussed and a convenient linearized form is obtained. The use of this form is shown to be entirely adequate.

The use of constant density models is discussed and it is shown that such models cannot explain all of the observational results for line-to-continuum ratios and line profiles. In particular, observations of high $n\alpha$ lines can be explained only in terms of models which contain extensive outer regions of low density.

A spherically symmetric model is constructed for the Orion nebula. The electron density $N_e$ is tabulated as a function of the distance $r$ from the centre, and the electron temperature is taken to be $9{\cdot}5 \times 10^3$°K. This model gives agreement with the following radio observations, to within observational errors: the total continuum flux as a function of frequency; all observed line-to-continuum ratios; all observed line profiles. The electron temperature is in good agreement with temperatures deduced from the relative intensities of forbidden lines. From the success achieved with this model it is concluded that the basic theory used for the interpretation of the recombination lines is correct. An essential feature of the theory is the assumption that $N_e$ decreases as $r$ increases. In order to take account of other observations, having higher angular resolution, it will be necessary to consider more complicated models, which allow for local fluctuations in $N_e$.


## 1. INTRODUCTION

The observation and interpretation of radio recombination lines constitutes an important branch of radio astronomy. Transitions in hydrogen have been detected over a wide range of frequencies, from 36·5 GHz ($n = 56 \rightarrow n = 55$) to 404 MHz ($n = 254 \rightarrow n = 253$). Many of these transitions have also been detected in helium. Although most of the observed lines are emitted in regions of ionized hydrogen ($H^+$ regions), recent work by Ball *et al.* (1970) provides convincing evidence that certain ' anomalous ' lines are due to transitions in carbon and are produced in regions of neutral hydrogen ($H^0$ regions) lying in front of $H^+$ regions.

There has been much discussion about the interpretation of the observations. Since the publication of the paper of Kardashev (1959), which predicted that the lines could be observed, the most important paper on the theory of recombination lines is that of Goldberg (1966), in which it is shown that maser action may enhance the line intensities. Subsequently a great deal of work has been done on the development of the basic atomic physics which is required for the precise quantitative interpretation of the observations. The theory of pressure broadening of the radio

lines has been developed by Griem (1967). In order to determine the amount of maser action it is necessary to calculate the populations of highly excited states, as functions of temperature and density, allowing for all relevant radiative and collisional processes. Percival & Richards (1969) have developed entirely new techniques for the calculation of cross sections for transitions between high excited states and estimate that, at temperatures occurring in $H^+$ regions, the calculated rate coefficients for these transitions should not be in error by more than 20 per cent. Using these rate coefficients, Brocklehurst (1970) has calculated the level populations and Brocklehurst & Leeman (1971) have recalculated the line-broadening parameters; their line-broadening results are in good agreement with the earlier results of Griem. The theory of line broadening has been further discussed by Peach (1972) who concludes that the errors in the results of Brocklehurst and Leeman should be no larger than the errors in the cross-sections of Percival and Richards.

In Sections 2–5 of the present paper we give a critical review of the basic atomic physics data required for the interpretation of the radio recombination lines. It is concluded that the possible errors in these data are fairly small and hence cannot give rise to any major source of uncertainty in discussions of the interpretation of the observations.

Attempts have been made to interpret the observed line-to-continuum ratios assuming models of constant electron density, $N_e$, and neglecting pressure broadening (the latest paper is that of Hjellming & Gordon 1971). It is found that large values of $N_e$ are required ($N_e \simeq 10^4$ cm$^{-3}$). These models cannot be entirely correct, since at these high densities the widths of the lines due to transitions between high quantum states would be nearly two orders of magnitude larger than the observed widths. Brocklehurst & Seaton (1971) have considered models in which $N_e$ decreases as a function of the distance $r$ from the centre of a nebula, and have obtained some encouraging results. Models of this type are discussed further in the present paper and it is shown that, for the Orion nebula, one can obtain close agreement with observations for line-to-continuum ratios, lines profiles, and total continuum fluxes.

In the present paper we do not consider the interpretation of observations which have good angular resolution. In particular, we do not consider the interpretation of surface brightness contours obtained at radio wavelengths using interferometric techniques, and we do not consider optical observations of doublet intensity ratios ([O II] and [S II]) which are sensitive to electron density. In order to obtain completely satisfactory interpretations of all of the available observations it will undoubtedly be necessary to consider more complicated models, which allow for fluctuations in $N_e$ at all values of $r$ (Hjellming, Andrews & Sejnowski 1969). So far as the interpretation of observations which do not have high angular resolution is concerned, we believe that it is essential to allow for the systematic variation of $N_e$ as a function of $r$, but of lesser importance to allow for the purely local fluctuations in $N_e$. In our opinion the success obtained with the Orion model of the present paper shows that the basic theory used for the interpretation of the recombination lines is correct.

## 2. THE RADIO CONTINUUM

For thermal sources the radio continuum is due to free–free processes,

$$X^+ + e \rightleftharpoons X^+ + e + h\nu. \qquad (2.1)$$

We consider that $X^+$ is either $H^+$ or $He^+$; in high excitation planetaries one must also consider the contribution from $He^{2+}$, but in the present paper this contribution is neglected.

Oster (1961) calculates the absorption coefficient for (2.1) using classical theory, and shows that quantum corrections are small. The expression obtained may be written

$$\kappa = N_e^2 r_e^3 \lambda^2 \times \left(\frac{8}{3\sqrt{(2\pi)}}\right)\left(\frac{mc^2}{kT}\right)^{3/2} \times \ln\left\{\left(\frac{2}{\gamma}\right)^{5/2}\left(\frac{kT}{mc^2}\right)^{3/2}\left(\frac{\lambda}{2\pi r_e}\right)\right\} \qquad (2.2)$$

where $T$ is the electron temperature, $r_e = e^2/(mc^2)$ is the electromagnetic radius of the electron, $\lambda = c/\nu$ is the wavelength and ln $(\gamma)$ is the Euler–Mascheroni constant, 0·5772 .... The electron density is $N_e = N(H^+) + N(He^+)$. Since the free electrons have a Maxwellian energy distribution the emissivity for the continuum is given by Kirchhoff's law,

$$j = \kappa B \qquad (2.3)$$

where $B = (2h\nu^3/c^2)/(\exp(h\nu/kT) - 1)$ is the Planck function. At radio wavelengths $(h\nu/kT) \ll 1$ and

$$B = (2\nu^2/c^2)\, kT. \qquad (2.4)$$

Inserting numerical values for the constants in (2.2) we obtain

$$\kappa = N_e^2 \times 6{\cdot}94 \times 10^{-8} \nu^{-2} (10^4/T)^{3/2} \{4{\cdot}69 + \tfrac{3}{2} \log (T/10^4) - \log \nu\} \qquad (2.5)$$

with $\kappa$ in $psc^{-1}$, $N_e$ in $cm^{-3}$, $\nu$ in GHz and $T$ in K.

The intensity $I$ for the continuum in a direction $\hat{\mathbf{n}}$ is obtained on solving the transfer equation

$$\frac{dI}{dx} = \kappa I - j \qquad (2.6)$$

where $x$ is a distance variable measured in the direction $-\hat{\mathbf{n}}$. Assuming $T$ to be constant, the solution for $I$ at a point $P$ is

$$I_P = B(1 - \exp(-\tau_P)) \qquad (2.7)$$

where

$$\tau_P = \int_{x_P}^{\infty} \kappa \, dx. \qquad (2.8)$$

The total optical depth of a nebula, along a line of sight in the direction towards the observer, is denoted by $\tau$:

$$\tau = \int_0^{\sigma} \kappa(s) \, ds \qquad (2.9)$$

where $s$ is the distance measured from the part of the nebula closest to the observer and $\sigma$ is the total length of the nebula along the line of sight. The total optical depth is proportional to the emission measure,

$$E = \int_0^{\sigma} N_e^2 \, ds. \qquad (2.10)$$

With $T$ constant, the observed intensity is

$$I = B(1 - \exp(-\tau)). \qquad (2.11)$$

## 3. FREQUENCIES, EMISSIVITIES AND ABSORPTION COEFFICIENTS FOR THE RADIO LINES

### 3.1 *Frequencies*

For level $n$ of hydrogen the energy is

$$E_n = -\chi_1/n^2 \tag{3.1}$$

where $\chi_1 = hRc$, $R$ being the Rydberg constant: $R = 109737{\cdot}31/(1+m/M_{\rm H})$ cm$^{-1}$ where $m$ is the electron mass and $M_{\rm H}$ the proton mass. For highly excited states of neutral atoms other than hydrogen, the same formula may be used with $M_{\rm H}$ replaced by the nuclear mass $M$.

For the line $n+m\rightarrow n$ the frequency is $\nu$ where

$$h\nu = \chi_1\{n^{-2}-(n+m)^{-2}\}. \tag{3.2}$$

For $n \gg 1$ and $m \ll n$ we obtain

$$h\nu = \chi_1 \frac{2m}{n^3}\left(1-\frac{3}{2}\frac{m}{n}+\ldots\right), \tag{3.3}$$

giving

$$\nu \simeq 6{\cdot}58m(100/n)^3 \text{ GHz}. \tag{3.4}$$

The lines are referred to as $n\alpha$, $n\beta$, $n\gamma$, ... for $m = 1, 2, 3, \ldots$.

### 3.2 *Emissivities and absorption coefficients*

The emissivity per unit volume for the line $n'\rightarrow n$ is

$$j_\nu^L = N_{n'}\frac{A_{n'n}}{4\pi}h\nu\phi_\nu \tag{3.5}$$

where $N_{n'}$ is the number of atoms per unit volume in level $n'$ and $A_{n'n}$ is the Einstein spontaneous emission coefficient. In (3.5), $\phi_\nu$ is a normalized profile factor,

$$\int \phi_\nu \, d\nu = 1. \tag{3.6}$$

Using the usual Einstein relations we obtain for the absorption coefficient, corrected for stimulated emission,

$$\kappa_\nu^L = \frac{c^2}{2\nu^2}\left[\frac{N_n}{\omega_n}-\frac{N_{n'}}{\omega_{n'}}\right]\omega_{n'}\frac{A_{n'n}}{4\pi}\phi_\nu \tag{3.7}$$

where $\omega_n$ is the statistical weight of level $n$.

The profile factors $\phi_\nu$ vary rapidly as functions of $\nu$. Our convention is to put subscripts $\nu$ only on quantities involving the factors $\phi_\nu$. We define $j^L$ and $\kappa^L$ to be emissivities and absorption coefficients integrated over frequency:

$$j^L = \int j_\nu^L \, d\nu, \quad \kappa^L = \int \kappa_\nu^L \, d\nu. \tag{3.8}$$

Using (3.6) it follows that

$$j_\nu^L = j^L\phi_\nu, \quad \kappa_\nu^L = \kappa^L\phi_\nu. \tag{3.9}$$

It is convenient to express $j^L$ and $\kappa^L$ in terms of the corresponding coefficients

for thermodynamic equilibrium, denoted by 'TE'. These coefficients satisfy the Kirchhoff relation,

$$j^L(\mathrm{TE}) = \kappa^L(\mathrm{TE})\, B. \tag{3.10}$$

Let us put

$$N_n = b_n N_n(\mathrm{TE}) \tag{3.11}$$

where $N_n(\mathrm{TE})$ is the number of atoms $X$ in level $n$ for Saha equilibrium:

$$N_n(\mathrm{TE}) = N_e N_+ \left(\frac{\omega_n}{2\omega_+}\right)\left(\frac{h^2}{2\pi mkT}\right)^{3/2} \exp\left(\chi_n/kT\right) \tag{3.12}$$

where $N_+ = N(\mathrm{X}^+)$, $(\omega_n/2\omega_+) = n^2$ and $\chi_n = \chi_1/n^2$.

The emissivity for the line $n' \to n$ is

$$j^L = b_{n'} j^L(\mathrm{TE}) \tag{3.13}$$

and the absorption coefficient is, in the notation of Goldberg (1966),

$$\kappa^L = b_n \beta_{n,n'} \kappa^L(\mathrm{TE}) \tag{3.14}$$

where

$$\beta_{n,n'} = \left(1 - \frac{b_{n'}}{b_n} \exp\left(-h\nu/kT\right)\right) \Big/ \left(1 - \exp\left(-h\nu/kT\right)\right). \tag{3.15}$$

Putting $n' = n + m$ and using the approximations

$$b_{n+m}/b_n = 1 + h\nu\, d(\ln b_n)/dE_n \tag{3.16}$$

$$\exp\left(-h\nu/kT\right) = 1 - h\nu/kT, \tag{3.17}$$

where $h\nu = E_{n+m} - E_n$, we obtain

$$\beta_{n,\,n+m} = 1 - kT \frac{d \ln b_n}{dE_n}. \tag{3.18}$$

This result is seen to be independent of $m$. Consistent with the approximations (3.16), (3.17) we may neglect the difference between $b_{n'}$ in (3.13) and $b_n$ in (3.14). Dropping subscripts $n$ we have

$$j^L = b j^L(\mathrm{TE}), \quad \kappa^L = b\beta\kappa^L(\mathrm{TE}) \tag{3.19}$$

$$\beta = 1 - kT\, d(\ln b)/dE. \tag{3.20}$$

It is convenient to express $\kappa^L(\mathrm{TE})$ in terms of the absorption oscillator strength $f$:

$$\kappa^L(\mathrm{TE}) = N_e N_+ \frac{\pi e^2}{mc} \left(\frac{h^2}{2\pi mkT}\right)^{3/2} n^2 \exp\left(\chi_n/kT\right) \frac{h\nu}{kT} f. \tag{3.21}$$

For $n \gg 1$ and $m \ll n$ it is shown by Menzel (1968) that

$$f = nK(m)\left\{1 + \frac{3}{2}\frac{m}{n} + \ldots\right\} \tag{3.22}$$

where $mK(m)$ is given in Table I. Using (3.3) we obtain

$$h\nu f = \chi_1 \frac{2mK(m)}{n^2}\left\{1 + O(m/n)^2\right\}. \tag{3.23}$$

TABLE I

*Values of $mK(m)$*

| $m$ | $mK(m)$ |
|---|---|
| 1 | 0·1908 |
| 2 | 0·05266 |
| 3 | 0·02432 |
| 4 | 0·01397 |
| 5 | 0·00906 |

The final result for the absorption coefficient may be written

$$\kappa_\nu^L(\mathrm{TE}) = N_e N_+ r_e a_0^3 \lambda \times \exp(\chi_n/kT)(\chi_1/kT)^{5/2} 16\pi^{5/2} \times mK(m) \times (\nu\phi_\nu) \qquad (3.24)$$

where $a_0 = \hbar^2/(mc^2)$ is the Bohr radius and where it should be noted that $(\nu\phi_\nu)$ is dimensionless. Inserting numerical values for the constants we obtain

$$\kappa_\nu^L(\mathrm{TE}) = N_e N_+ \times 1{\cdot}064 \times 10^{-12} \times \nu^{-1}(10^4/T)^{5/2} \times mK(m) \exp(\chi_n/kT)(\nu\phi_\nu) \qquad (3.25)$$

with units as in (2.5). We have $(\chi_n/kT) = 15{\cdot}79(10^4/n^2T)$; the factor $\exp(\chi_n/kT)$ in (3·25) is therefore close to unity and may usually be omitted.

3.3 *Calculation of the departure coefficients $b_n$*

It is shown by Brocklehurst (1971) that collisional redistribution of angular momentum is very effective for the highly excited states, and hence that $b_{nl} = b_n$.

The level populations $N_n$ are calculated on solving a system of equations

$$\mathbf{KN} = \mathbf{R} \qquad (3.26)$$

where $\mathbf{N}$ is a vector with components $N_n$, $R_n$ gives the number of captures per unit volume per unit time on level $n$, and $\mathbf{K}$ is a matrix obtained on allowing for all transitions between atomic energy levels and for ionization.

Brocklehurst (1970) has solved the equations

$$\mathbf{K}^{(0)}\mathbf{N} = \mathbf{R} \qquad (3.27)$$

where $\mathbf{K}^{(0)}$ is calculated allowing for: spontaneous emission; redistribution of energy by electron impact and ionization by electron impact: and $\mathbf{R}$ is calculated allowing for radiative recombination and three-body recombination (inverse of electron-impact ionization). The factors $b$ differ from unity because much of the radiation produced in a nebula can freely escape. The calculations of Brocklehurst have been made for the usual two cases: for Case A it is assumed that all radiation can freely escape; and for Case B it is assumed that radiation due to transitions to the ground state is re-absorbed. For the highly excited states there is no great difference between the calculations for these two cases. For most nebulae it can be assumed that Case B applies. Brocklehurst tabulates the quantities $b$ and

$$C = -\log d \ln b/dn.$$

Putting $dE_n = (2\chi_1/n^3)\,dn$ we have, using (3.20) $\beta = 1-(kT/\chi_1)(n^3/2)\,d(\ln b)/dn$, giving

$$\log(1-\beta) = \log(T/10^4) + 3\log n - C - 1{\cdot}50. \qquad (3.28)$$

Fig. 1 shows $b$ as a function of $(E_n/\chi_1) = -1/n^2$ and Fig. 2 shows $\log(1-\beta)$ as a function of $n$; these results are for $T = 10^4$K and $\log N_e = 2$, 3 and 4.

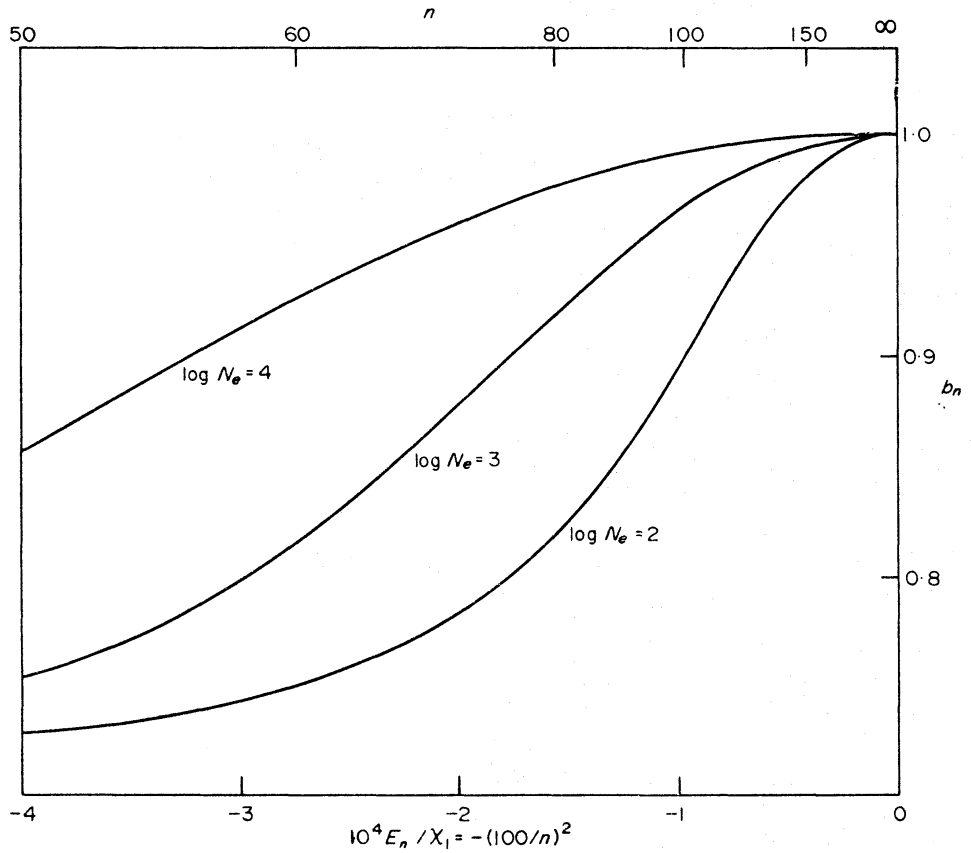


FIG. 1. *Values of* $b_n$ *against* $10^4\, E_n/\chi_1 = -(100/n)^2$, for $T = 10^{4\cdot0}K$ and *log* $N_e = 2$, 3 and 4, *with* $N_e$ *in* $cm^{-3}$ (*from Brocklehurst* 1970).

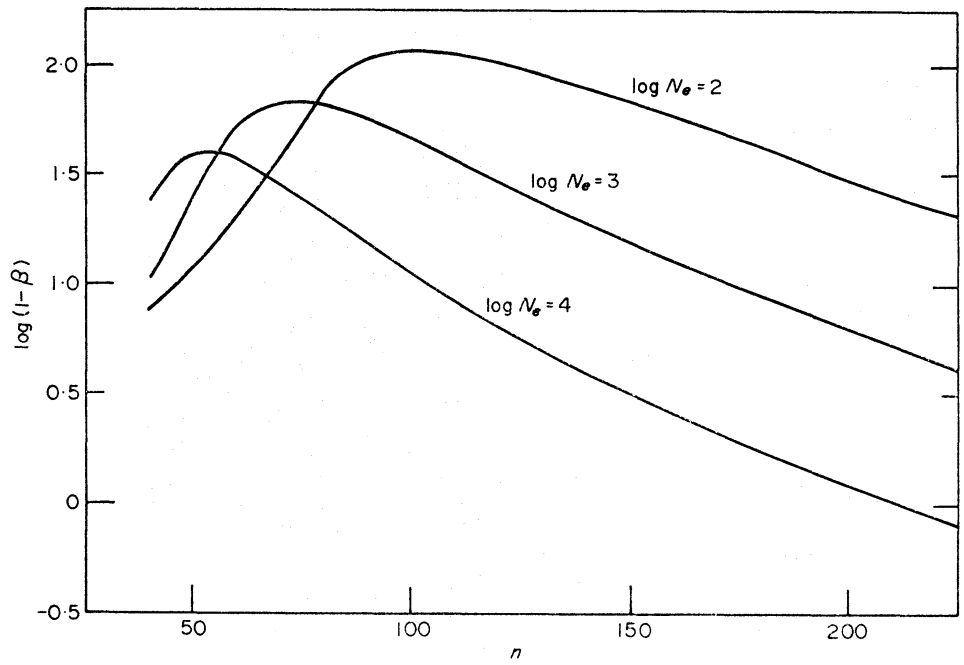


FIG. 2. *Values of log* $(1-\beta)$ *against n for* $T = 10^{4\cdot0}K$ *and log* $N_e = 2$, 3 *and* 4, *with* $N_e$ *in* $cm^{-3}$ (*from the results of Brocklehurst* 1970).

The equations (3.27) have been solved assuming an infinite number of quantized levels (we shall return to this point in Section 5) and to a numerical accuracy of 0·1 per cent in $(1-\beta)$.

### 3.4 *Absorption of radiation*

At radio frequencies the intensity in the continuum is always large compared with the intensities in the lines. From (2.5) it is seen that the continuum absorption coefficient $\kappa$ is proportional to $\nu^{-2}$ and that the optical depth $\tau$ must become large in the limit of $\nu$ small; the continuum intensity $I$ then approaches the Planck intensity $B$ (see (2.7)). In practice this condition is approached only for the intensities of high $n\alpha$ lines. For a highly excited state the transition probability for emission of an $n\alpha$ photon is small compared with the total radiative transition probability. For these reasons we would not expect the absorption of radiation to be a process of major importance in the calculation of level populations, but some further checks can be made.

Dyson (1969) has calculated level populations allowing for absorption of radiation, and assuming constant-density models. This gives two cases.

(i) For models with high density and high emission measure, collisions are very effective and absorption of radiation turns out to be of little importance.

(ii) For models with low density and low emission measure the continuum intensity is small and again absorption of radiation is of little importance.

So long as one considers models of constant density, the case of low density and high emission measure does not arise, since this would give unreasonably large linear dimensions $\sigma$.

We shall consider models of variable density and we must therefore estimate the effect of absorption of radiation in regions of low density in front of regions of high emission measure. In (3.26) let us put

$$\mathbf{K} = \mathbf{K}^{(0)} + \mathbf{K}^{(1)} \tag{3.28}$$

where $\mathbf{K}^{(0)}$ is the matrix used by Brocklehurst (1970) and $\mathbf{K}^{(1)}$ allows for absorption of continuum radiation in spectrum lines; $\mathbf{K}^{(1)}$ is proportional to the mean radiation intensity,

$$J = \frac{1}{4\pi}\int I\, d\omega. \tag{3.29}$$

We assume that $\mathbf{K}^{(1)}$ is small and that (3.26) can be solved by iteration:

$$\mathbf{K}^{(0)}\mathbf{N}^{(0)} = \mathbf{R} \tag{3.30}$$

$$\mathbf{K}^{(0)}\mathbf{N}^{(1)} = \mathbf{R} - \mathbf{K}^{(1)}\mathbf{N}^{(0)} \text{ etc.} \tag{3.31}$$

where (3.30) has been solved by Brocklehurst (1970). We have

$$(\mathbf{K}^{(1)}\mathbf{N}^{(0)})_n = \sum_{n'>n}\left(\frac{4\pi\kappa^L J}{h\nu}\right)_{n\to n'} - \sum_{n'<n}\left(\frac{4\pi\kappa^L J}{h\nu}\right)_{n'\to n} \tag{3.32}$$

where $\kappa^L$ is calculated using $\mathbf{N}^{(0)}$. For a low density region in front of a high density region of optical depth $\tau$ we may use the approximation

$$J = \tfrac{1}{2}B(1-e^{-\tau}). \tag{3.33}$$

For all lines except high $n\alpha$ lines $J$ will be much smaller than $B$. Considering only absorption in $n\alpha$ lines ($n' = n \pm 1$) we have

$$(\mathbf{K}^{(1)}\mathbf{N}^{(0)})_n = G_n - G_{n-1} \simeq \frac{dG_n}{dn} \tag{3·34}$$

where

$$G_n = \left(\frac{4\pi\kappa^L J}{h\nu}\right)_{n\to n+1}. \tag{3·35}$$

It follows that the solution $\mathbf{N}^{(1)}$ of (3·31) will differ little from the solution $\mathbf{N}^{(0)}$ of (3·30) if

$$\left|\frac{dG_n/dn}{R_n}\right| \ll 1. \tag{3·36}$$

Fig. 3 gives values of $(dG_n/dn)/R_n$ for a region with $N_e = 10^2$ cm$^{-3}$ in front of regions with emission measures of $1 \times 10^7$ and $2 \times 10^7$ cm$^{-6}$ psc. It is seen that

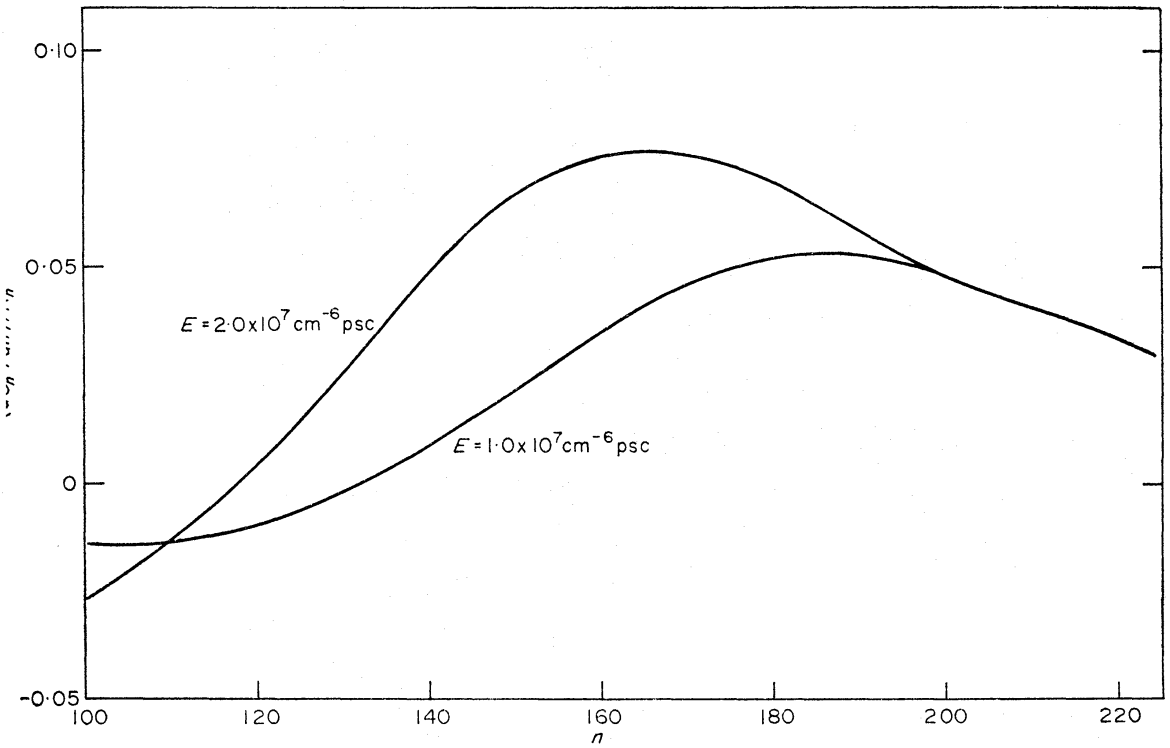


FIG. 3. *Values of* $(dG_n/dn)/R_n$ *against n for a region with* $T = 10^4K$, $N_e = 10^2$ *cm*$^{-3}$ *in front of a region with emission E. Results for* $E = 1 \times 10^7$ and $2 \times 10^7$ *cm*$^{-6}$ *psc.*

absorption of radiation never gives a perturbation larger than 8 per cent of the processes taken into account in the zero-order approximation. We may therefore conclude that, even for this case, absorption of continuum radiation is not an important process.

## 4. LINE PROFILES

The profile factors $\phi_\nu$ are obtained on convoluting profiles $\phi_\nu^D$ for Doppler broadening with profiles $\phi_\nu^P$ for pressure broadening:

$$\phi_\nu = \int \phi^P_{\nu-\nu'+\nu_0}\phi^D_{\nu'}\, d\nu' \tag{4·1}$$

where $\nu_0$ is the frequency of the line centre. The Doppler broadening is due to both thermal and non-thermal motions. We assume a gaussian Doppler profile,

$$\phi_\nu{}^D = \frac{\alpha}{\pi^{1/2}\nu_0} \exp\{-[\alpha(\nu-\nu_0)/\nu_0]^2\} \tag{4.2}$$

where

$$\alpha = [Mc^2/(2kT_D)]^{1/2} \tag{4.3}$$

and where $T_D$ is the ' Doppler temperature '.

The pressure broadening is due to quasi-static electric fields (Stark effect) and to collisions (impact effect). Griem (1967) shows that the impact effect is more important than the Stark effect and that electron impacts are more important than proton impacts. We therefore neglect the Stark effect and proton impacts. We assume a Lorentz profile for broadening by electron impacts, giving $\phi_\nu{}^P = \phi_\nu{}^I$ where

$$\phi_\nu{}^I = \frac{\delta}{\pi}\{(\nu-\nu_0)^2+\delta^2\}^{-1} \tag{4.4}$$

Brocklehurst & Leeman (1971) calculate $\delta$ as

$$\delta = \frac{1}{2\pi}\langle vQ\rangle N_e \tag{4.5}$$

where $Q$ is the total inelastic cross-section and $\langle\ \rangle$ denotes an average over the Maxwellian distribution. The results obtained may be fitted to

$$\delta = 4{\cdot}7(n/100)^{4{\cdot}4}(10^4/T)^{0{\cdot}1}\, N_e \text{ Hz}. \tag{4.6}$$

Using a more exact theory, Peach (1972) shows that the Lorentz form (4.4) is not strictly correct but that the use of (4.4) and (4.5) does not lead to errors greater than about 10 per cent.

Let $\Delta\nu$ be the full width of the profile at half-maximum ($\phi_{\nu_1} = \frac{1}{2}$ where $\nu_1 = \nu_0 + \frac{1}{2}\Delta\nu$). The Doppler profile (4.2) gives a width $(\Delta\nu)^D$ such that

$$\frac{(\Delta\nu)^D}{\nu_0} = 1{\cdot}009\times 10^{-4}\left\{\frac{M_H}{M}\times\frac{T_D}{2\times 10^4}\right\}^{1/2} \tag{4.7}$$

and the impact profile (4.4) gives a width $(\Delta\nu)^I = 2\delta$. For $n\alpha$ lines we obtain

$$\frac{(\Delta\nu)^I}{\nu_0} = 1{\cdot}43\times 10^{-5}\left(\frac{n}{100}\right)^{7{\cdot}4}\left(\frac{10^4}{T}\right)^{0{\cdot}1}\left(\frac{N_e}{10^4}\right). \tag{4.8}$$

Considering the case of $H\ n\alpha$ lines with $T = 1\times 10^4$ and $T_D = 2\times 10^4$ we have

$$\frac{(\Delta\nu)^I}{(\Delta\nu)^D} = 0{\cdot}142(n/100)^{7{\cdot}4}\left(\frac{N_e}{10^4}\right). \tag{4.9}$$

With $N_e = 10^4$ cm$^{-3}$ this gives $(\Delta\nu)^I/(\Delta\nu)^D \simeq 50$ for 220$\alpha$. Since densities of order $10^4$ cm$^{-3}$ certainly occur in gaseous nebulae, it is clear that impact broadening must be an important process.

Convoluting the Doppler profile (4.2) with the impact profile (4.4),

$$\phi_\nu = \frac{\alpha}{\pi^{1/2}\nu_0} H(a, x) \tag{4.10}$$

where $a = \alpha\delta/\nu_0$, $x = \alpha(\nu-\nu_0)/\nu_0$ and

$$H(a, x) = \frac{a}{\pi}\int_{-\infty}^{+\infty}\frac{e^{-t^2}\,dt}{a^2+(t-x)^2} \tag{4.11}$$

is the Voigt function.

## 5. ACCURACY OF THE ATOMIC DATA

In various discussions of the interpretation of the radio recombination lines it has been suggested that discrepancies between theory and observations might be due to errors in the atomic data which have been used. The accuracy of these data has been discussed in the preceding sections of the present paper, but there is one further point which must be checked.

The highly excited states are perturbed by other particles, and as the quantum number $n$ becomes sufficiently large it is no longer permissible to assume the existence of quantized states of the free atom. As a first approximation, we may consider that there is some value $n_q$ of $n$ such that quantized states exist for $n<n_q$ but not for $n>n_q$. The value of $n_q$ will, of course, depend on $T$ and $N_e$. The level populations $N_n$ calculated assuming an infinite number of quantized levels will be accurate only for $n\ll n_q$.

From the work of Griem (1967) it follows that collisions will be more important than the Stark effect in perturbing the quantized states. In order to estimate the value of $n_q$ we compare the time taken for an electron to complete a Bohr orbit with the mean time between collisions. The orbit time is

$$\mathscr{P}_n = 2\pi r_n/v_n \tag{5.1}$$

where $r_n$ is the radius of the orbit and $v_n$ the electron velocity. The time between collisions is

$$\mathscr{C}_n = 1/(\langle vQ\rangle N_e). \tag{5.2}$$

Since the quantized state will certainly not exist if a collision occurs before the electron can complete one orbit, we take

$$\mathscr{P}_n \simeq \mathscr{C}_n \quad \text{for} \quad n = n_q. \tag{5.3}$$

Using the Bohr theory of the hydrogen atom it may be shown that $\mathscr{P}_n \simeq 1/\nu_{n\alpha}$ where $\nu_{n\alpha}$ is the frequency of the $n\alpha$ line. Using (4.5) we obtain $\mathscr{C}_n = 1/(\pi(\Delta\nu)^I)$ where $(\Delta\nu)^I$ is the line width due to impact broadening. The condition (5.3) is therefore equivalent to

$$(\Delta\nu)^I/\nu_{n\alpha} \simeq 1/\pi \quad \text{for} \quad n = n_q. \tag{5.4}$$

From observations of the lower $n\alpha$ lines, which are not significantly broadened by electron impacts, one obtains $(\Delta\nu)^D/\nu \simeq 10^{-4}$. The observed widths of the high $n\alpha$ lines never exceed about $2\times(\Delta\nu)^D$. For the impact widths we therefore obtain $(\Delta\nu)^I/\nu \lesssim 10^{-4}$. From (4.8) and (5.4) it therefore follows that $(n/n_q)^{7.4} \lesssim \pi\times 10^{-4}$ giving $n \lesssim 0{\cdot}3 n_q$ for the regions in which the observed lines are formed. From this result it may be concluded that there will not be any large error in the level populations calculated assuming an infinite number of quantized levels.

Our general conclusion is that possible errors in the atomic data used for the interpretation of the recombination lines are no larger than the errors which

typically occur in the observational results. If results are calculated assuming a particular model for the structure of a nebula, and if the difference between calculated and observed results is large compared with the probable errors in the observations, then it must be concluded that some incorrect assumptions have been made in constructing the model.

## 6. SOLUTIONS OF THE TRANSFER PROBLEM

### 6.1 *General formulation*

We shall use the term ' absorption of radiation ' to mean both true absorption and stimulated emission; both are included in the coefficients $\kappa$ and $\kappa_\nu^L$. Although it has been shown in Section 3.4 that absorption is not a process of major importance for the determination of the level populations, it follows from the work of Goldberg (1966) that absorption can be of great importance for the calculation of the intensities of the observed lines. The first step in the construction of models is therefore to obtain a suitable approximate form for the solutions of the equations of radiative transfer.

On solving the transfer equation (3.6) we obtain for the emergent intensity in the continuum

$$I = \int_0^\sigma j\, e^{-t}\, ds \tag{6.1}$$

where $s$ is the distance along the line of sight, measured from the part of the source closest to the observer, and where $\sigma$ is the total length of the source along the line of sight. In (6.1)

$$t(s) = \int_0^s \kappa(s')\, ds'. \tag{6.2}$$

The intensity for line-plus-continuum is

$$I_\nu^L + I = \int_0^\sigma (j + j_\nu^L)\, e^{-t-t_\nu^L}\, ds \tag{6.3}$$

where

$$t_\nu^L(s) = \int_0^s \kappa_\nu^L(s')\, ds'. \tag{6.4}$$

The intensity in the line is therefore

$$I_\nu^L = \int_0^\sigma \{(j + j_\nu^L)\, e^{-t_\nu^L} - j\}\, e^{-t}\, ds. \tag{6.5}$$

### 6.2 *Approximate expressions*

We simplify (6.5) on making three approximations.

*Approximation* (i) is to assume $|t_\nu^L| \ll 1$. Let $\tau_{\nu_0}^L = t_{\nu_0}^L(\sigma)$ where $\nu_0$ is the frequency of the line centre. Fig. 4 shows $\log(-\tau_{\nu_0}^L)$ for $n\alpha$ lines, calculated for models which have constant electron density $N_e$ and emission measures $E = N_e^2\sigma$. For all cases considered $\tau_{\nu_0}^L$ is negative. It is seen that $|\tau_{\nu_0}^L|$ is never larger than 0·03. Putting $\exp(-t_\nu^L) = 1 - t_\nu^L$, (6.5) reduces to

$$I_\nu^L = \int_0^\sigma \{j_\nu^L - (j + j_\nu^L)\, t_\nu^L\}\, e^{-t}\, ds. \tag{6.6}$$

*Approximation* (ii) is to assume $j_\nu^L \ll j$. Fig. 5 shows $j_\nu^L(\mathrm{TE})/j$ for $n\alpha$ lines; this ratio depends only on electron temperature and gives an upper limit for $j_\nu^L/j$. It is seen that $j_\nu^L \ll j$ is a good approximation for $n > 100$, less good for $n < 100$. Using this approximation, (6.6) reduces to

$$I_\nu^L = \int_0^\sigma \{j_\nu^L - j t_\nu^L\} \, \mathrm{e}^{-t} \, ds. \tag{6.7}$$

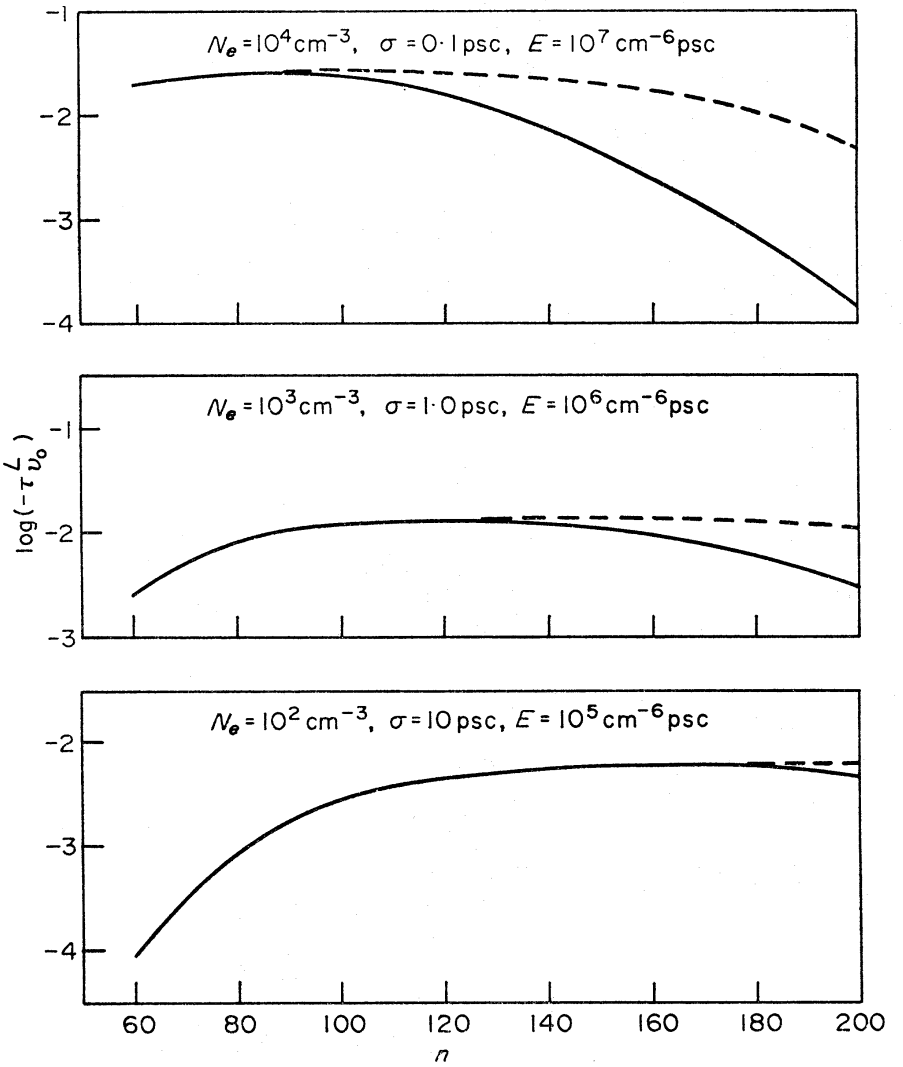


FIG. 4. *Values of* $\log(-\tau_{\nu_0}{}^L)$ *against n, where* $\tau_{\nu_0}{}^L$ *is the line optical depth at the centre of* $n\alpha$ *lines. Results are given for three models of different density and emission measure. All calculations for* $T = 1 \times 10^{4\circ}K$, $T_D = 2 \times 10^{4\circ}K$. ——— *calculations allowing for impact broadening*; – – – *calculations neglecting impact broadening.*

*Approximation* (iii) is to assume $T$ to be constant. Some variations in $T$ may occur but we do not expect them to be large or to have any particularly important effects on the calculated line intensities. To simplify (6.7) we use $t$ as independent variable: using (2.3) we obtain

$$I_\nu^L = \int_0^\tau \left\{\frac{j^L}{\kappa} - B t_\nu^L\right\} \mathrm{e}^{-t} \, dt \tag{6.8}$$

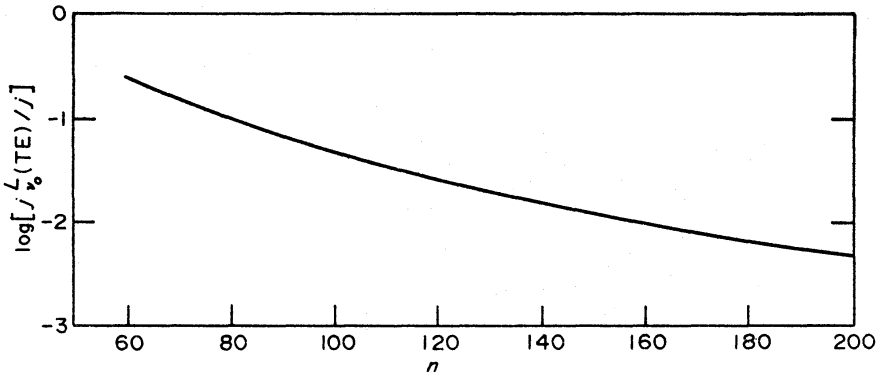


FIG. 5. *Values of $j_{\nu_0}{}^L(TE)/j$ against n, where $j_{\nu_0}{}^L(TE)$ is the emissivity at the centre of an nα line assuming thermodynamic equilibrium, and j is the emissivity for the continuum at the nα line frequency. All calculations for $T = 1 \times 10^4 K$, $T_D = 2 \times 10^4 K$, and neglecting impact broadening.*

where

$$t_\nu{}^L = \int_0^s \kappa_\nu{}^L \, ds' = \int_0^t \frac{\kappa_\nu{}^L}{\kappa} \, dt'. \tag{6.9}$$

We put $j_\nu{}^L = j^L(\mathrm{TE}) b\phi_\nu = B\kappa^L(\mathrm{TE}) b\phi_\nu$ (using (3.10)) and $\kappa_\nu{}^L = \kappa^L(\mathrm{TE}) b\beta\phi_\nu$. At constant $T$, $B$ is constant and $\kappa^L(\mathrm{TE})/\kappa$ is constant; (6.8) therefore reduces to

$$I_\nu{}^L = B \frac{\kappa^L(\mathrm{TE})}{\kappa} y_\nu \tag{6.10}$$

where

$$y_\nu = \int_0^\tau \left\{ b\phi_\nu - \int_0^t b\beta\phi_\nu \, dt' \right\} \mathrm{e}^{-t} \, dt. \tag{6.11}$$

On integrating by parts we obtain

$$y_\nu = \int_0^\tau \{\mathrm{e}^{-\tau} + (1-\beta)(\mathrm{e}^{-t} - \mathrm{e}^{-\tau})\} b\phi_\nu \, dt. \tag{6.12}$$

It should be noted that this expression is linear in the profile factor $\phi_\nu$. On integrating over the frequency of a line we have

$$I^L = B \frac{\kappa^L(\mathrm{TE})}{\kappa} y \tag{6.13}$$

where

$$y = \int_0^\tau \{\mathrm{e}^{-\tau} + (1-\beta)(\mathrm{e}^{-t} - \mathrm{e}^{-\tau})\} \, b \, dt. \tag{6.14}$$

We may put

$$I_\nu{}^L = I^L \theta_\nu \tag{6.15}$$

where $\theta_\nu$ is the normalized profile factor for the observed line:

$$\int \theta_\nu \, d\nu = 1 \tag{6.16}$$

and

$$\theta_\nu = y_\nu / y. \tag{6.17}$$

It should be noted that we have $\theta_\nu = \phi_\nu$ only for models of constant density or for lines which have negligible impact broadening.

### 6.3 *Discussion of the approximate expressions*

Let us consider the factor

$$\{e^{-\tau}+(1-\beta)(e^{-t}-e^{-\tau})\} \tag{6.18}$$

in (6.12) and (6.14). First, we note that both terms, $e^{-\tau}$ and $(1-\beta)(e^{-t}-e^{-\tau})$, are always positive. Next, we consider the case that $\beta = 1$, so that there is no maser action; in this case (6.18) reduces to $e^{-\tau}$ which gives a reduction in line intensity due to absorption. Finally we consider the term $(1-\beta)(e^{-t}-e^{-\tau})$ which gives an increase in line intensity due to maser action. For two reasons this term is most important for small values of $t$, that is to say for those parts of the source closest to the observer. The first reason is that $(e^{-t}-e^{-\tau})$ is largest for small $t$; the line is mased by the continuum intensity in the direction towards the observer and this intensity is largest for those parts of the source closest to the observer. The second reason is that low densities may be expected in the outer regions, and $(1-\beta)$ generally increases as the density decreases (see Fig. 2). We shall see later that a third effect, the density dependence of the profile factors $\phi_\nu$, may also be important for the high lines.

### 6.4 *Accuracy of the approximations*

In order to obtain a check on the accuracy of Approximations (i) and (ii) of Section 6.2, we expand the integrand of (6.5) in powers of $\phi_\nu$, to obtain

$$I_\nu{}^L = [I_\nu{}^L]^{(1)}+[I_\nu{}^L]^{(2)}+\ldots \tag{6.19}$$

where

$$[I_\nu{}^L]^{(1)} = \int_0^\sigma \{j_\nu{}^L - jt_\nu{}^L\}\, e^{-t}\, ds \tag{6.20}$$

is the expression (6.7) linear in $\phi_\nu$ and where

$$[I_\nu{}^L]^{(2)} = -\int_0^\sigma t_\nu{}^L \{j_\nu{}^L - \tfrac{1}{2}jt_\nu{}^L\}\, e^{-t}\, ds \tag{6.21}$$

is a correction term quadratic in $\phi_\nu$. The error introduced by using Approximations (i) and (ii) will be small if $|\mathscr{R}_\nu{}^L| \ll 1$ where

$$\mathscr{R}_\nu{}^L = [I_\nu{}^L]^{(2)}/[I_\nu{}^L]^{(1)}. \tag{6.22}$$

We evaluate $\mathscr{R}_\nu{}^L$ for a model of constant temperature and constant density. After some straightforward reductions we obtain

$$\mathscr{R}_\nu{}^L = -\left\{\tau_\nu{}^L \int_0^\tau t(1-\tfrac{1}{2}\beta t)\, e^{-t}\, dt\right\}\Big/\left\{\tau \int_0^\tau (1-\beta t)\, e^{-t}\, dt\right\}$$

$$= -\frac{\tau_\nu{}^L}{2}\left\{\frac{1+2(1-\beta)[e^\tau-1-\tau-\tfrac{1}{2}\tau^2]/\tau^2}{1+(1-\beta)[e^\tau-1-\tau]/\tau}\right\}. \tag{6.23}$$

The largest values of $\mathscr{R}_\nu{}^L$ occur for $n\alpha$ lines and for nebulae with large emission measures. Considering the case of $E = 2\times 10^7$ cm$^{-6}$ psc and $N_e \simeq 10^4$ cm$^{-3}$ we find that the largest value of $\mathscr{R}_\nu{}^L$, $\mathscr{R}_\nu{}^L = 0{\cdot}03$, occurs at about $90\alpha$. At $110\alpha$ we have $\mathscr{R}_\nu{}^L = 0{\cdot}02$. These values are for the line centre. Away from the centre the error will be smaller. We may conclude that, to within the accuracy of present day observations, the Approximations (i) and (ii) of Section 6.2 are entirely adequate.

Approximation (iii) is made as a matter of convenience and because we do not expect temperature variations to be a factor of major importance for the interpretation of the observations; the theory can easily be generalized to the case in which the temperature is variable.

### 6.5 *Line-to-continuum intensity ratios*

Assuming $T$ to be constant the continuum intensity is given by (2.11) and the line-to-continuum intensity ratios by

$$\frac{I_\nu^L}{I} = \frac{I^L}{I}\theta_\nu, \quad \frac{I^L}{I} = \frac{\kappa^L(\mathrm{TE})}{\kappa} Y \tag{6.24}$$

where

$$Y = y/(1-\mathrm{e}^{-\tau}). \tag{6.25}$$

The ratio $I^L/I$ has dimensions of frequency and is usually given in units of kHz. The factor $Y$ is dimensionless. From (2.5) and (3.25) we obtain

$$\frac{\kappa^L(\mathrm{TE})}{\kappa} = \frac{N_+}{N_\mathrm{e}} \times 1{\cdot}533 \times 10^{-5}\nu^2 \left(\frac{10^4}{T}\right) mK(m) \times \left\{4{\cdot}69 + \frac{3}{2}\log\frac{T}{10^4} - \log\nu\right\}^{-1} \mathrm{kHz} \tag{6.26}$$

with $\nu$ in GHz. In the present paper we shall assume a He/H abundance ratio of 0·10 and suppose that all the He is singly ionized; we then have $N(\mathrm{H}^+)/N_e = 1/1{\cdot}1$.

The observers usually measure the aerial temperatures, $T_L$ and $T_C$, at the line centre and in the adjacent continuum, and the full width of the line at half maximum intensity, $\Delta\nu$. Assuming a gaussian profile factor $\theta_\nu$ for the observed line, one obtains

$$\frac{I^L}{I} = \frac{1}{2}\left(\frac{\pi}{\ln 2}\right)^{1/2} \Delta\nu \, \frac{T_L}{T_C}. \tag{6.27}$$

For a given line, $\kappa^L(\mathrm{TE})/\kappa$ depends only on electron temperature. The observed ratios may be analysed in one of the following ways.

(i) If the electron temperature is assumed to be known we may deduce $Y$. This is such that $Y = 1$ for a nebula which is optically thin ($\tau \ll 1$) and in TE ($b = \beta = 1$).

(ii) We may define an effective temperature $T^*$ such that

$$\frac{I^L}{I} = \left\{\left(\frac{\kappa^L(\mathrm{TE})}{\kappa}\right) \text{ calculated for a temperature } T^*\right\}. \tag{6.28}$$

This is such that $T = T^*$ for an optically thin nebula in TE. If (6.27) is also used a further assumption is implied: that impact broadening is not important.

(iii) Given a complete theoretical model of the structure of a nebula we may calculate the ratios $I^L/I$ and compare with the observed ratios.

## 7. MODELS OF CONSTANT DENSITY

It is instructive to begin by considering models of constant density although, in view of the remarks made at the end of Section 6.2, it is evident that such models may not be satisfactory for the interpretation of observations of real nebulae.

### 7.1 *Expressions for* Y

From (6.14) and (6.25) we obtain, for models of constant density,

$$Y = b\{f(\tau) + (1-\beta)[1-f(\tau)]\} \tag{7.1}$$

where $f(\tau) = \tau/(e^{\tau}-1)$ is shown in Fig. 6. We have two limiting cases: (i) for $\tau \ll 1$,

$$Y = b\{1 + \tfrac{1}{2}(1-\beta)\,\tau\} \qquad (\tau \ll 1) \tag{7.2}$$

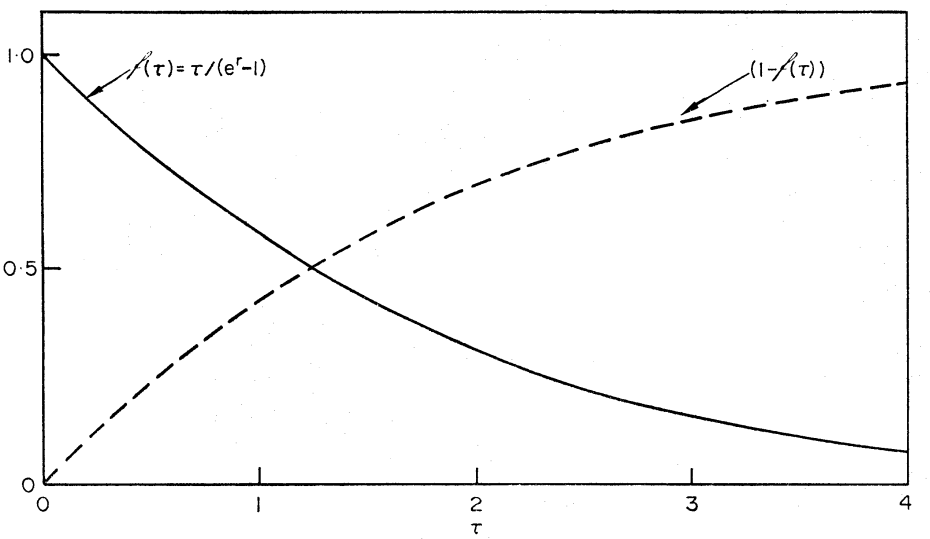


FIG. 6. *The functions* $f(\tau) = \tau/(e^{\tau}-1)$, *and* $(1-f(\tau))$, *against* $\tau$.

(it should be noted that we do not assume $(1-\beta)\,\tau \ll 1$ since we may have $(1-\beta) \gg 1$); (ii) for $\tau \gg 1$,

$$Y = b(1-\beta) \qquad (\tau \gg 1) \tag{7.3}$$

which implies that the lines are produced entirely by maser action.

### 7.2 *Electron temperatures*

It is possible to observe a number of lines, $n+m \rightarrow n$, all at nearly the same frequency; thus, for example, Davies (1971) has made observations for Orion of the lines 110$\alpha$, 138$\beta$, 158$\gamma$, 173$\delta$ and 186$\epsilon$ all at frequencies close to 4·9 GHz. At this frequency $\tau$ is small and (7.2) may be assumed. As $n$ and $m$ increase we have $b \rightarrow 1$ and $\beta \rightarrow 1$ (see Figs 1 and 2). In this limit we therefore have $T^* \rightarrow T$. Fig. 7 shows $T^*$ deduced from the observations of Davies. It is seen that $T^*$ tends to a value of about $10^4$°K, which is in satisfactory agreement with temperatures deduced from forbidden lines (Peimbert & Costero 1969). A similar analysis has been made by Hjellming & Davies (1970). We shall tentatively assume that $T = 10^4$°K for Orion. An attempt to obtain a more exact value will be described in Section 9.

### 7.3 *Interpretation of* n$\alpha$ *lines*

Fig. 8 shows values of $Y$ deduced from Orion observations of $\Delta\nu T_L/T_C$,

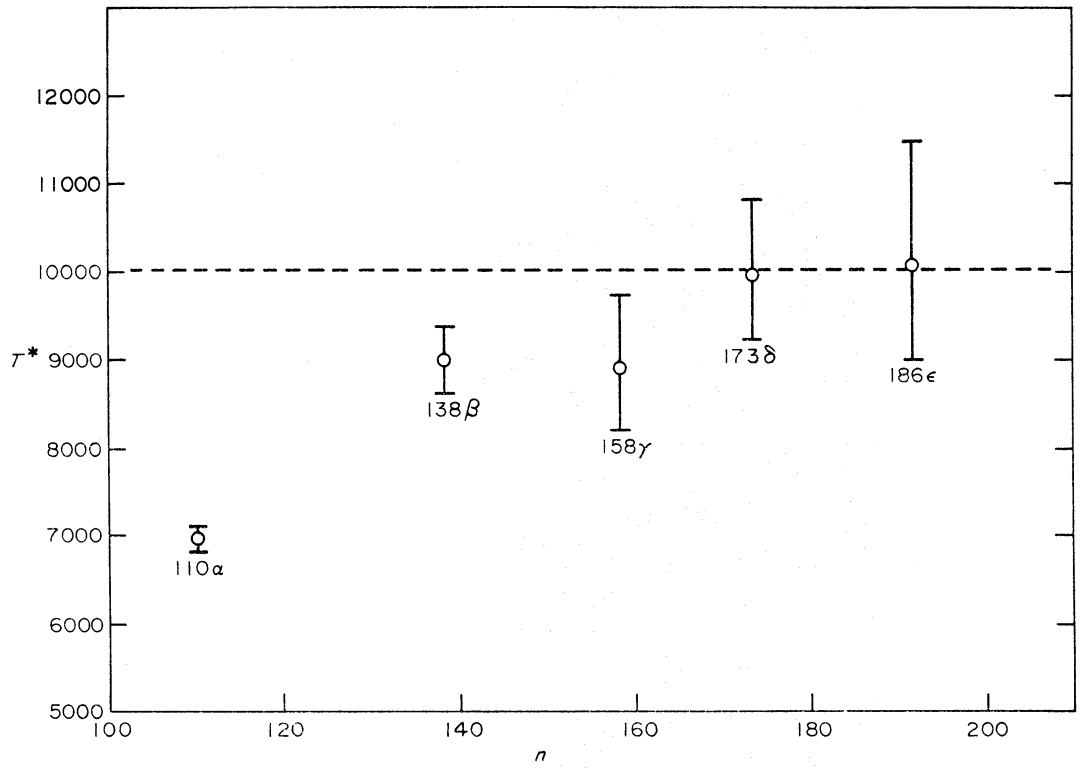


FIG. 7. *Values of T* (defined by* (6.28)) *against n, obtained from line observations of Davies* (1971) *for Orion at frequencies close to* 4·9 *GHz.*

assuming $T = 10^4$°K. We use the data quoted by† Hjellming & Gordon (1971), together with an additional point obtained by Pedlar (1971) for 220α.

Let us first consider the high $n\alpha$ lines. In this limit we expect to have $\tau \gg 1$ and hence the expression (7.3) for $Y$. It should be noted that this gives $Y$ to depend only on electron density $N_e$. We obtain the best agreement with observations for $N_e = 2 \times 10^4$ cm$^{-3}$.

We now consider the lower $n\alpha$ lines, for which we may assume $\tau \ll 1$ and hence the expression (7.2) for $Y$. Given $N_e$ the observations may be used to deduce $\tau$ and hence the emission measure $E$; the best fit is obtained with $E = 2{\cdot}1 \times 10^7$ cm$^{-6}$ psc. The complete function $Y$ calculated with $N_e = 2 \times 10^4$ cm$^{-3}$ and $E = 2{\cdot}1 \times 10^7$ cm$^{-6}$ psc is shown on Fig. 8. Our results for the constant density model are in agreement with those of Hjellming and Davies, although we differ in the methods of analysis and presentation.

The following points should be noted. The intensities of the high lines are determined entirely by maser action. For these lines the values of $Y$ deduced from observation are not large, and we must therefore assume a high density, $N_e$; with a smaller value of $N_e$ we would obtain calculated values of $Y$ which would be too large (see Fig. 2). For the lower lines the observations give $Y$ to be significantly greater than unity. With large values of $N_e$, $(1-\beta)$ in (7.2) is small and one must take $E$ to be large in order to obtain agreement with observations.

† Hjellming and Gordon quote a value of $\Delta\nu T_L/T_C$ for 85α from Gordon (1970) which is not in agreement with the value given in Gordon's paper. Dr Gordon informs us that the value given in the original paper is correct.

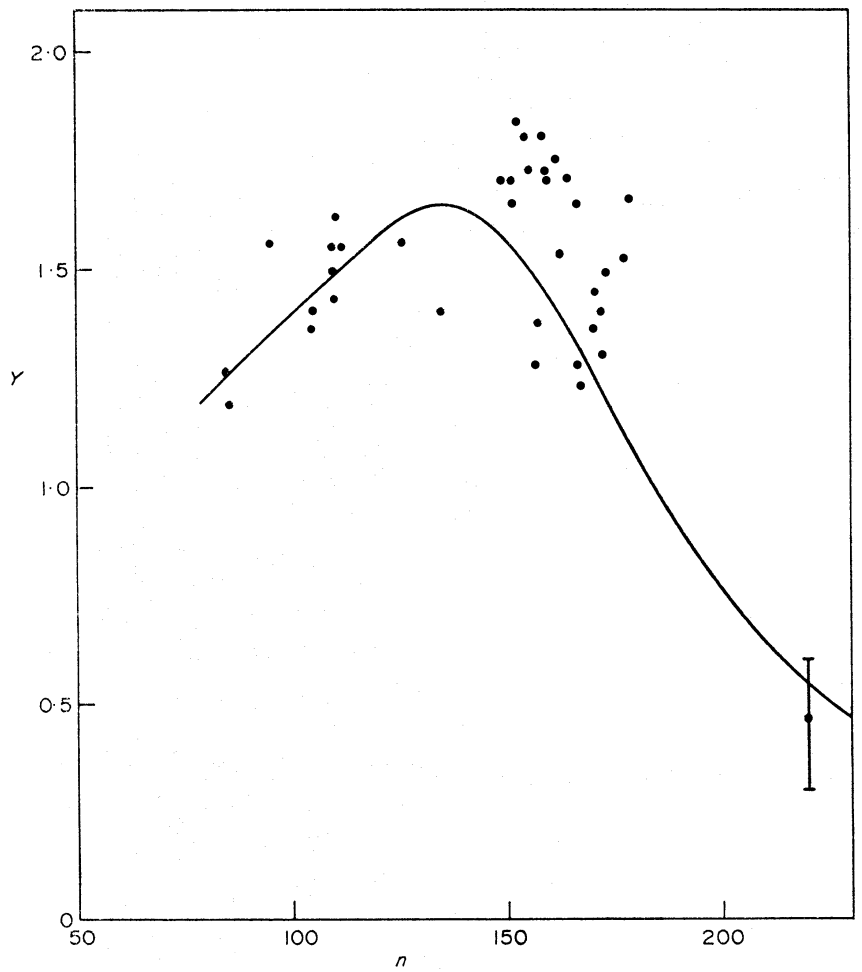


FIG. 8. *Values of Y deduced from observations of nα lines in Orion, assuming* $T = 1 \times 10^4$°K. *The curve ——— is calculated for a model of constant density,* $N_e = 2 \times 10^4$ *cm*$^{-3}$, *and emission measure* $E = 2{\cdot}1 \times 10^7$ *cm*$^{-6}$ *psc.*

### 7.4 *Line profiles*

Let $\Delta\nu$ be the total width of a line and $(\Delta\nu)^D$ the corresponding Doppler width. From observations of the lower $n\alpha$ lines one obtains $T_D = 2 \times 10^4$°K for Orion. Using (4.9) and assuming $N_e = 2 \times 10^4$ cm$^{-3}$ we calculate $\Delta\nu/(\Delta\nu)^D \simeq 100$ for 220$\alpha$. The observations of Pedlar & Davies (1971) show that $\Delta\nu/(\Delta\nu)^D$ for 220$\alpha$ in Orion does not exceed 1·7. We therefore conclude that the constant density models cannot be correct for the interpretation of the high lines.

### 7.5 *Continuum intensities*

A further reason for not accepting the model with $E = 2{\cdot}1 \times 10^7$ cm$^{-6}$ psc, $N_e = 2 \times 10^4$ cm$^{-3}$ is that it does not give agreement with observations for the continuum intensity as a function of frequency.

## 8. MODELS OF VARIABLE DENSITY

The observed profiles show that the high $n\alpha$ lines must be produced in regions of low density. In a previous paper (Brocklehurst & Seaton 1971) we have suggested that all of the line observations can be understood using models of variable density.

In order to illustrate the ideas involved we consider a simple model containing two regions, denoted by superscripts (1) and (2). Region (1) is closest to the observer. We take the parameters for the two regions to be: $N_e^{(1)} = 10^2$ cm$^{-3}$ and $\sigma^{(1)} = 2{\cdot}0$ psc giving $E^{(1)} = 2\times 10^4$ cm$^{-6}$ psc; and $N_e^{(2)} = 10^4$ cm$^{-3}$ and $\sigma^{(2)} = 0{\cdot}1$ psc giving $E^{(2)} = 10^7$ cm$^{-6}$ psc. Table II gives the continuum optical depths, $\tau^{(1)}$ and $\tau^{(2)}$, at the frequencies of $n\alpha$ lines. It is seen that

$$\tau^{(1)} \ll 1 \quad \text{and} \quad \tau^{(1)} \ll \tau^{(2)}. \tag{8.1}$$

TABLE II

*Optical depths at frequencies of $n\alpha$ lines for the model of Section 8, containing two regions*

| Line | $\tau^{(1)}$ | $\tau^{(2)}$ |
|---|---|---|
| 100α | 0·0001 | 0·06 |
| 140α | 0·0010 | 0·52 |
| 180α | 0·0051 | 2·54 |
| 220α | 0·0179 | 8·94 |

Integrating (6.12) we obtain

$$y_\nu = (b\phi_\nu)^{(1)}\{\tau^{(1)}\,e^{-\tau} + (1-\beta)^{(1)}[1 - e^{-\tau^{(1)}} - \tau^{(1)}\,e^{-\tau}]\}$$
$$+ (b\phi_\nu)^{(2)}\{\tau^{(2)}\,e^{-\tau} + (1-\beta)^{(2)}[e^{-\tau^{(1)}} - (1+\tau^{(2)})\,e^{-\tau}]\} \tag{8.2}$$

where $\tau = \tau^{(1)} + \tau^{(2)}$. The line to continuum ratio is

$$\frac{I_\nu^L}{I} = \frac{\kappa^L(\mathrm{TE})}{\kappa}\,Y_\nu \tag{8.3}$$

where $Y_\nu = y_\nu/(1-e^{-\tau})$. Using (8.2) we obtain

$$Y_\nu = (b(1-\beta)\,\phi_\nu)^{(1)}\tau^{(1)} + (b\phi_\nu)^{(2)}\{\not{f}(\tau) + (1-\beta)^{(2)}[1-\not{f}(\tau)]\} \tag{8.4}$$

with $\not{f}(\tau) = \tau/(e^\tau - 1)$. We now consider two lines, 100α and 220α.

100α. The profiles $\phi_\nu^{(1)}$ and $\phi_\nu^{(2)}$ are both close to the Doppler profile $\phi_\nu^D$. With $\tau \ll 1$, (8.4) reduces to

$$Y_\nu \simeq \{(b(1-\beta)^{(1)}\tau^{(1)} + b^{(2)} + (b(1-\beta))^{(2)}\tau^{(2)}\}\,\phi_\nu^D \text{ for } 100\alpha. \tag{8.5}$$

From Table II and Figs 1 and 2 we obtain $(b(1-\beta))^{(1)}\tau^{(1)} = 0{\cdot}01$, $b^{(2)} = 1{\cdot}0$ and $(b(1-\beta))^{(2)}\tau^{(2)} = 0{\cdot}6$. It is seen that region (1) contributes less than 1 per cent of the intensity of the 100α line.

200α. With $\tau \gg 1$ (8.4) reduces to

$$Y_\nu \simeq (b(1-\beta)\,\phi_\nu)^{(1)}\tau^{(1)} + (b(1-\beta)\,\phi_\nu)^{(2)} \text{ for } 220\alpha. \tag{8.6}$$

We obtain $(b(1-\beta))^{(1)}\tau^{(1)} = 0{\cdot}36$ and $(b(1-\beta))^{(2)} = 0{\cdot}80$. It follows that 31 per cent of the integrated 220α line intensity comes from region (1). However, the line profiles for the two regions are very different; using (4.9) we obtain $(\Delta\nu^I/\Delta\nu^D)^{(1)} = 0{\cdot}48$ and $(\Delta\nu^I/\Delta\nu^D)^{(2)} = 48{\cdot}0$. Thus the 220α line formed in region (1) has a profile similar to that of the observed line, while the line formed in region (2) will be so broad that it will not be observed. Considering only the contribution from region (1) we have $Y = 0{\cdot}36$, which is comparable with the observed value of $Y$ for 220α in Orion.

For models of this type the formation of high $n\alpha$ lines may be described as follows: the high density inner regions produce strong continuum radiation,

together with very broad lines which will not be detected; the continuum from the inner regions produces very effective maser action in the low density outer regions. The lines formed in the outer regions have narrow profiles and small values of $Y$, in agreement with observations.

## 9. A SECOND APPROXIMATION TO A MODEL FOR THE ORION NEBULA

Model C of our previous paper (Brocklehurst & Seaton 1971) was described as a first approximation to a model for the Orion nebula; it gave agreement with the main trends of the observational results for line-to-continuum ratios and line profiles, but no attempt was made to adjust the parameters of the model so as to obtain a best fit to the observations. We have subsequently constructed a more refined model which gives agreement, to within the accuracy of the observational results, for the following radio data for Orion A: the total continuum flux from 100 MHz to 36 GHz; all observed line-to-continuum ratios; all observed line profiles. We describe this model as a second approximation. It does not yet come close to a definitive model, since we do not attempt to fit to observational data which have high angular resolution.

### 9.1 *Description of the model*

We assume the electron temperature $T$ to be constant. The model is spherically symmetric and the electron density is assumed to depend only on $r$, the distance from the centre. We consider spheres of radius $r_i$, such that $r_0 = 0$ and $r_i > r_{i-1}$. Within the spherical shell $r_{i-1} < r < r_i$ the electron density is assumed to have a constant value $N_e^{(i)}$. We define $\Delta E^{(i)} = (N_e^{(i)})^2(r_i - r_{i-1})$. The total emission measure for a line of sight passing through the centre is then

$$E = 2 \sum_i \Delta E^{(i)}. \tag{9.1}$$

Let $\phi$ be the angular radius. We assume Orion to be at a distance of 450 psc; $\phi = 1'$ of arc then corresponds to $r = 0{\cdot}131$ psc.

### 9.2 *The computer program*

The coefficients $b_n$ and $C_n$, calculated by Brocklehurst (1970) for certain fixed values of $T$ and $N_e$, are stored on a permanent file. Values of these coefficients for any required values of $T$ and $N_e$ are computed using interpolation formulae. The following data are provided as input to the computer program: the temperature $T$, assumed to be constant; the distance of the nebula; the densities $N_e^{(i)}$ within each spherical shell and the increments in emission measure $\Delta E^{(i)}$; a list of lines for which calculations are required. For each line the program computes the fluxes

$$(F_\nu^L)^i = 2\pi \int_0^{\phi_i} I_\nu^L \phi \, d\phi \tag{9.2}$$

where $\phi_i$ is the angular radius of a shell, and the fluxes

$$(F)^i = 2\pi \int_0^{\phi_i} I\phi \, d\phi \tag{9.3}$$

for the adjacent continuum. The Voigt function is computed using a routine

supplied by Dr G. Rybicki, which proves to be very efficient. With eight shells the program takes 10 s, on the IBM 360/65 at University College London, to calculate the quantities (9.2) and (9.3) for one line.

Calculations were first made with $T = 10^4$°K and the density distribution varied so as to obtain a best fit to observations. It was found that close agreement could be obtained but that some small systematic discrepancies remained. Keeping the same density distribution, $T$ was then varied and it was found that the residual discrepancies with observations could be eliminated on taking $T = 9{\cdot}5 \times 10^3$°K. The parameters for the model are given in Table III.

TABLE III

*A second approximation to a model for the Orion nebula*

| Region $i=$ | $N_e^{(i)}$ Units $10^4$ cm$^{-3}$ | $\Delta E^{(i)}$ Units $10^6$ cm$^{-6}$ psc | $r_i - r_{i-1}$ psc | $r_i$ psc | $\phi_i$ ′ | ″ |
|---|---|---|---|---|---|---|
| 1 | 1·50 | 1·000 | 0·0044 | 0·0044 | 0 | 2 |
| 2 | 1·00 | 3·000 | 0·0300 | 0·0344 | 0 | 16 |
| 3 | 0·50 | 3·000 | 0·1200 | 0·1544 | 1 | 11 |
| 4 | 0·20 | 0·400 | 0·1000 | 0·2544 | 1 | 57 |
| 5 | 0·10 | 0·150 | 0·1500 | 0·4044 | 3 | 5 |
| 6 | 0·05 | 0·040 | 0·1600 | 0·5644 | 4 | 19 |
| 7 | 0·02 | 0·015 | 0·3750 | 0·9394 | 7 | 11 |
| 8 | 0·01 | 0·008 | 0·8000 | 1·7394 | 13 | 17 |

$T = 9{\cdot}5 \times 10^3$°K.
$E = 1{\cdot}52 \times 10^7$ cm$^{-3}$ psc for a line of sight through the centre.
Angular radii $\phi_i$ calculated assuming a distance of 450 psc.

## 9.3 *The total continuum radio flux*

The total continuum flux is

$$S = 2\pi \int I\phi \, d\phi \qquad (9.4)$$

where the integration is over the entire nebula. Table IV gives the calculated results and Fig. 9 compares the calculated results with observations. The observational data are taken from Hjellming & Churchwell (1969).

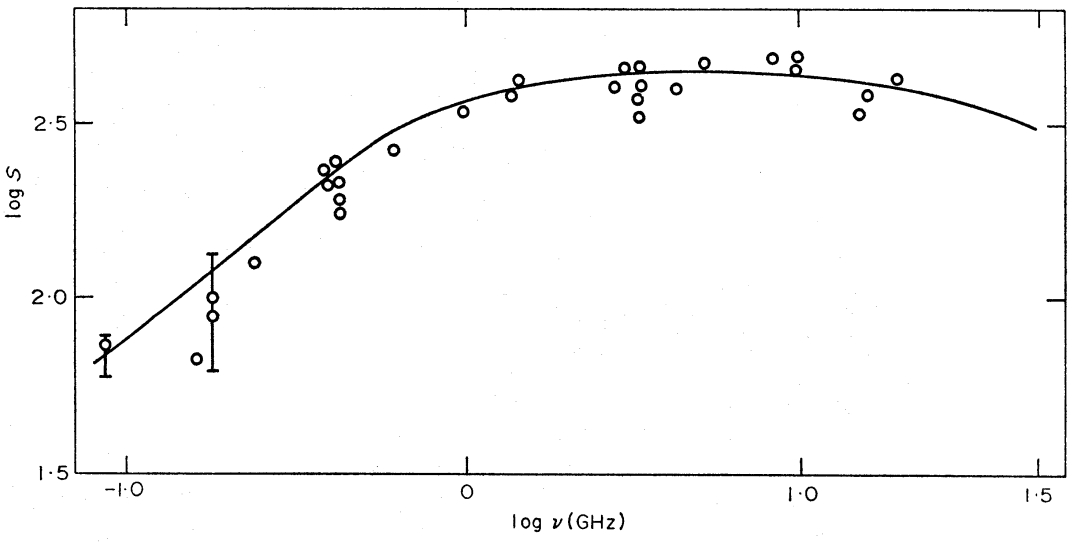


FIG. 9. *Values of total continuum flux for Orion A. Observed values,* o *and* ō. *Calculated results using model of Table III,* ———.

TABLE IV

*Calculated total continuum fluxes for the Orion model*

| $\nu$ GHz | $S$ f.u. ($10^{-26}$ W m$^{-2}$ Hz$^{-1}$) |
|---|---|
| 36·46 | 339 |
| 10·52 | 397 |
| 5·01 | 425 |
| 2·70 | 431 |
| 1·42 | 393 |
| 0·83 | 319 |
| 0·61 | 275 |
| 0·245 | 158 |
| 0·10 | 75 |

## 9.4 *The radio lines*

The calculated line intensities and profiles vary with position. At high frequencies the half-power beam widths, $\phi_{\mathrm{HPBW}}$, used by most observers are smaller than the total angular size of the nebula, while at lower frequencies the entire nebula is observed. In order to simplify the comparisons between theory and observations, we have adopted typical values of $\phi_{\mathrm{HPBW}}$ as functions of frequency; the adopted values are given in Table V. We make the further simplifying assumptions that all

TABLE V

*Values of $\phi_{\mathrm{HPBW}}$ assumed for Orion line observations*

| Line | $\nu$ GHz | $\phi_{\mathrm{HPBW}}$ ′ |
|---|---|---|
| 85α | 10·52 | 1·5 |
| 109α | 5·01 | 3 |
| 134α | 2·70 | 6 |
| 166α | 1·42 | 8 |
| 200α | 0·83 | 12 |
| 220α | 0·61 | 15 |

observations are made with the centre of the beam directed towards the centre of the nebula, and that all intensity is collected for $\phi < \phi_{\mathrm{HPBW}}$, none for $\phi > \phi_{\mathrm{HPBW}}$; the observed flux is then

$$F_\nu^L = 2\pi \int_0^{\phi_{\mathrm{HPBW}}} I\phi \, d\phi. \tag{9.5}$$

(i) *Line profiles.* We obtain agreement with the observed profiles for the lower hydrogen lines on taking $T_D = 2 \times 10^4$°K. In discussing profiles it is convenient to use the frequency variable

$$x = \alpha(\nu - \nu_0)/\nu_0 \tag{9.6}$$

where $\alpha = [Mc^2/(2kT_D)]^{1/2}$ (for H lines with $T_D = 2 \times 10^4$°K, $\alpha = 1{\cdot}65 \times 10^4$), and to define the profile factors

$$f(x) = F_\nu^L / F_{\nu_0}^L. \tag{9.7}$$

For pure Doppler broadening we then have $f(x) = \exp(-x^2)$.

Fig. 10 shows the computed profiles for H $n\alpha$ lines. It is seen that the high $n\alpha$

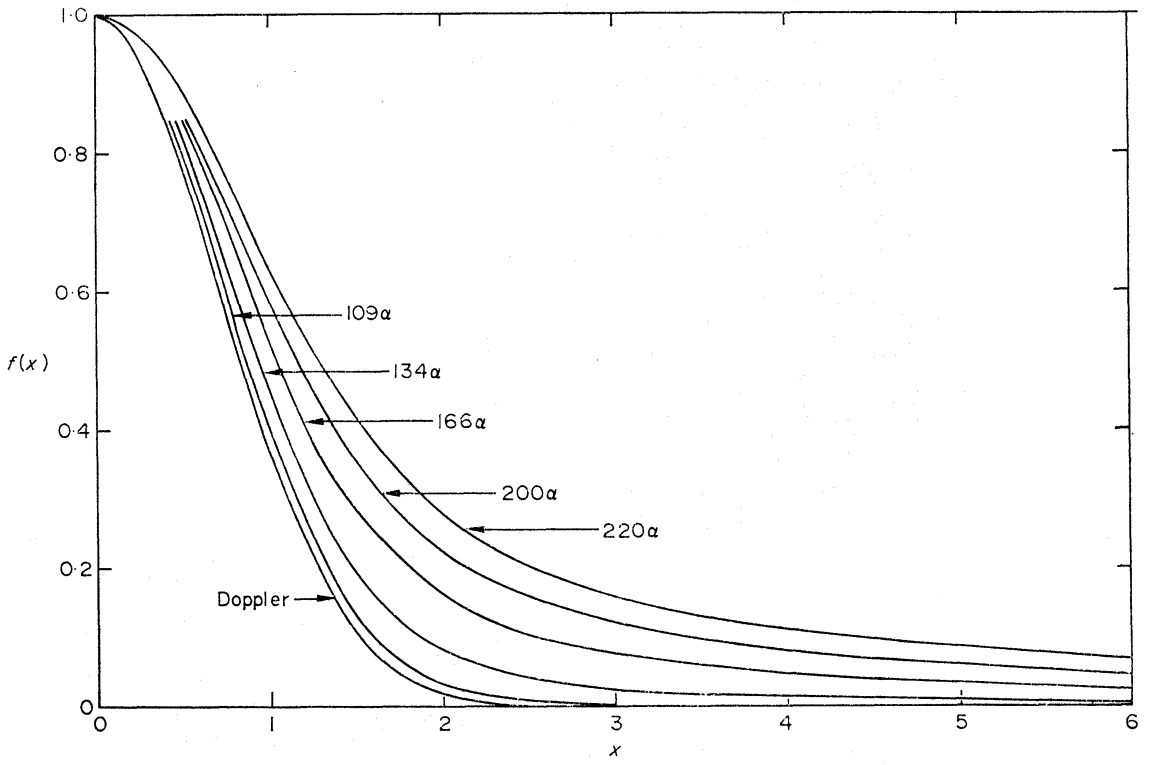


FIG. 10. *Computed profiles $f(x)$ for $n\alpha$ lines in Orion.*

lines have very broad wings. We believe that, due to the techniques which have been used, most observers have failed to detect these line wings, but we note that Simpson (1970) has detected broad wings in 168α. With high gain amplifiers used for line studies, the instrument sensitivity varies fairly rapidly as a function of frequency. The procedure of ' baseline subtraction ' used by most observers is to assume that, for $|x|$ greater than some value $x_0$, the observed signal is due to the continuum alone. Over the small frequency range considered in line work, the continuum intensity may be assumed to be independent of frequency. The variation of signal with $x$, for $|x| > x_0$, is therefore assumed to be a purely instrumental effect; the signal for $|x| > x_0$ is therefore fitted to a polynomial in $x$ and the part which varies with $x$ is subtracted from the observations in order to obtain the ' observed ' line profile. It is seen that broad line wings can easily be subtracted away along with the baselines.

In order to compare calculated line widths with observations, we subtract ' baselines ' from the computed profiles. In the line wings we fit $f(x)$ to $g(x) = p/(q^2+x^2)$ and compare the observed profiles with

$$f'(x) = [f(x)-g(x)]/[f(0)-g(0)]. \qquad (9.8)$$

Fig. 11 shows that the calculated widths $\Delta\nu$ of $n\alpha$ lines are in satisfactory agreement with observations. The observation of high $n\alpha$ lines are of interest in providing information about the low density outer regions. Fig. 12 shows how the computed profile of the 220α line varies as the width, $r_8$–$r_7$, of the outer region, with density $10^2$ cm$^{-3}$, is reduced by a factor $\xi$.

Profiles of the lines 109α, 137β, 157γ and 172δ, all at frequencies close to 5 GHz, have been measured by Churchwell (1971). Fig. 13 shows the computed profiles

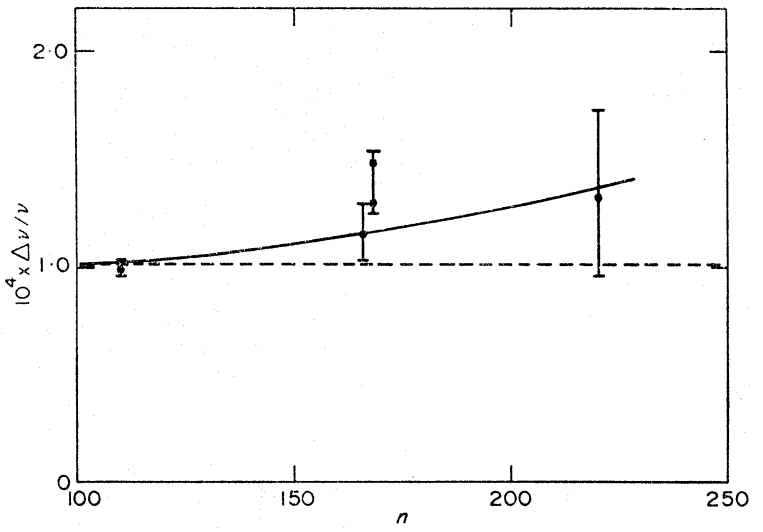


FIG. 11. *Values of $\Delta\nu/\nu$ for $n\alpha$ lines in Orion. Observed points:* 110α (*Davies* 1970); 166α (*Pedlar & Davies* 1971); 168α (*Simpson* 1970); 220α (*Pedlar & Davies* 1971). *Calculated results;* ———, *using model of Table III and ' baseline subtraction ' procedures discussed in text;* – – –, *for $T_D = 2 \times 10^4 K$ and no impact broadening.*

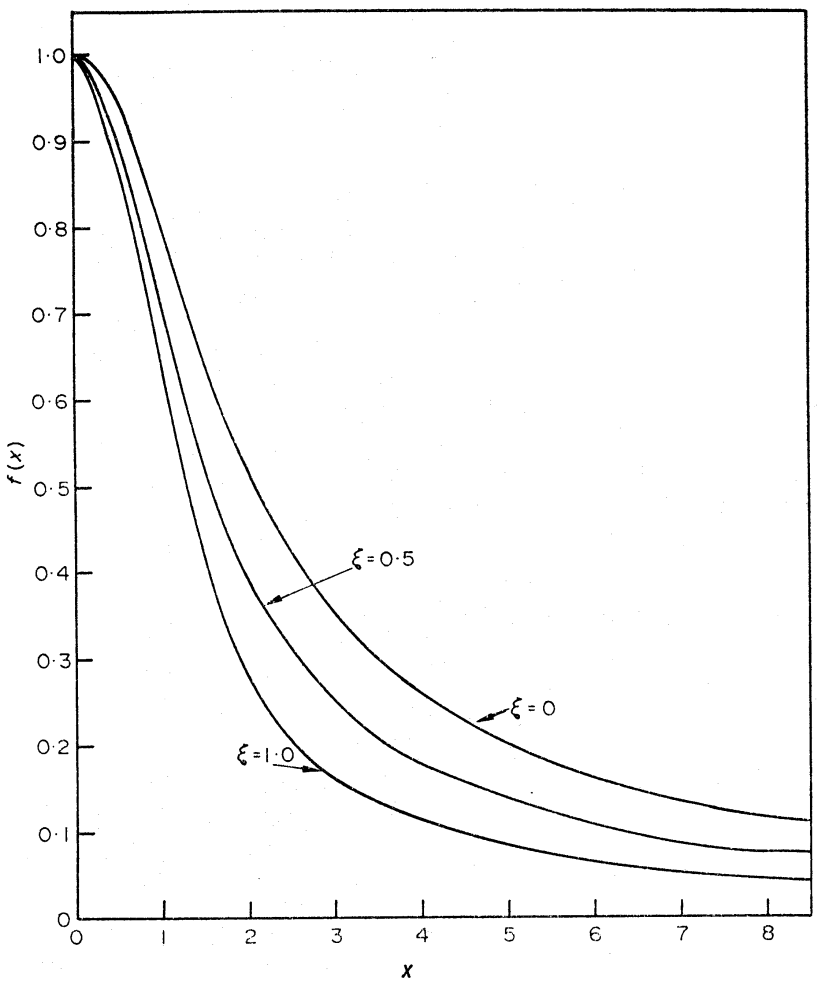


FIG. 12. *The computed profiles of 220α when the width, $r_8$–$r_7$, of the outer region of the model of Table III is reduced by a factor $\xi$.*

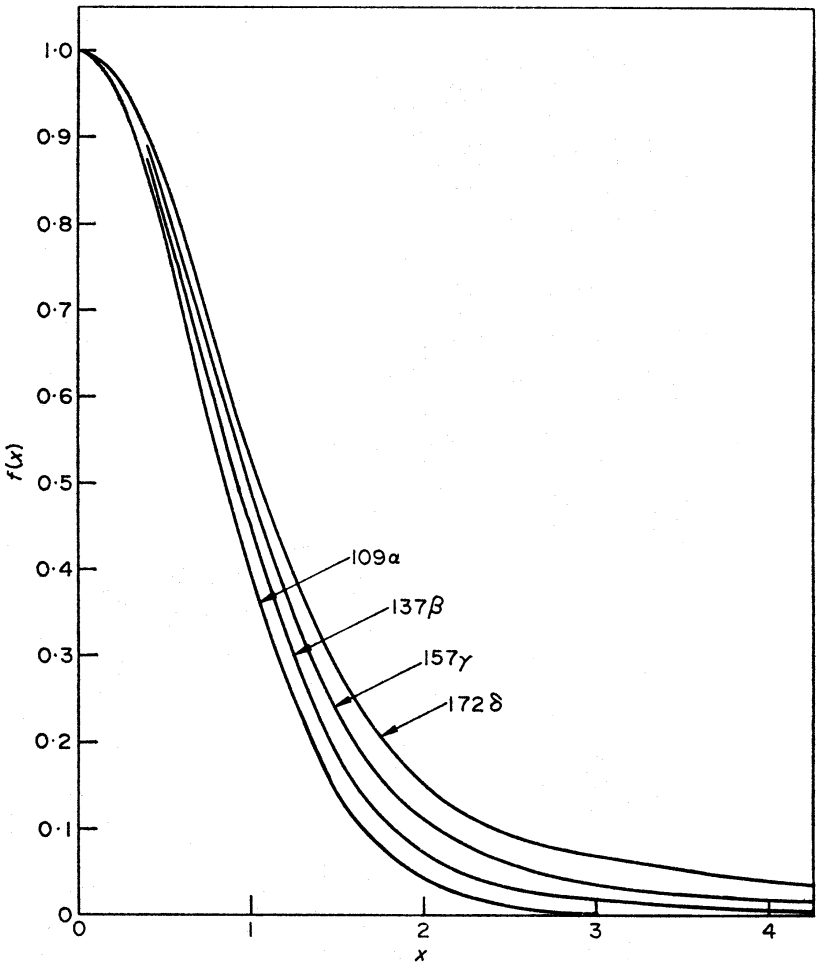


FIG. 13. *Profiles for the lines* 109α, 137β, 157γ *and* 172δ *at frequencies close to* 5 *GHz, calculated using the Orion model of Table III.*

for these lines, and Fig. 14 compares observed and calculated line widths. Since the procedure of baseline subtraction is somewhat arbitrary, we give two calculated curves: one with no baseline subtraction and one with what we judge to be a maximum baseline subtraction. The calculations are seen to agree with observations to within probable observational errors.

(ii) *Line-to-continuum ratios.* We first consider $n\alpha$ lines. The line-to-continuum ratios vary over several orders of magnitude, mainly due to the factor $\nu^2$ in (6.26). In previous comparisons between theory and observations, $\Delta\nu T_L/T_C$ has usually been plotted on a logarithmic scale. We feel that it is better to take out the rapidly varying factor, and we therefore consider the quantity $\nu^{-2}\Delta\nu T_L/T_C$. Let $(I^L/I)_{\text{calc}}$ be the calculated line to continuum ratio. In order to allow for baseline subtraction, we multiply by a factor

$$X = \int [f(x)-g(x)]\,dx \Big/ \int f(x)\,dx. \tag{9.9}$$

Using (6.27) we then have

$$\left(\Delta\nu \frac{T_L}{T_C}\right)_{\text{calc}} = 2\left(\frac{\ln 2}{\pi}\right)^{1/2}\left(X\frac{I^L}{I}\right)_{\text{calc}}. \tag{9.10}$$

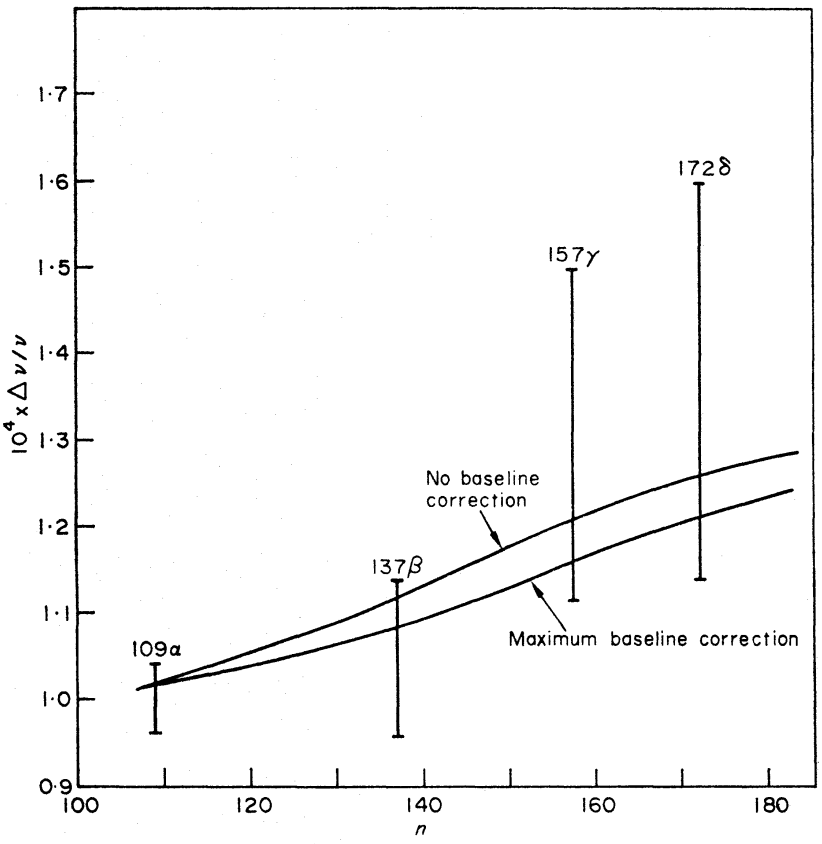


FIG. 14. *Widths for the lines* 109α, 137β, 157γ *and* 172δ *at frequencies close to* 5 *GHz* (*Churchwell* 1971). *Calculations for the model of Table III are given for two cases, no baseline subtraction and maximum baseline subtraction.*

Fig. 15 shows the observational results for $n\alpha$ lines in Orion (references are given in Section 7.3), together with calculated results for $T = 10^4$°K and $9{\cdot}5 \times 10^3$°K. The adopted values of $X$ are given in Table VI.

TABLE VI

*Values of baseline correction factors X for the model of Table III*

| Line | $X$ |
|---|---|
| 85α | 1·00 |
| 109α | 1·00 |
| 134α | 0·91 |
| 166α | 0·71 |
| 200α | 0·45 |
| 220α | 0·27 |

Next we consider sets of lines $(n+m)\rightarrow n$ all observed with the same telescope and at nearly the same frequency. Here the main variation in line-to-continuum ratios is due to the factor $mK(m)$ in (6.26); we therefore consider the quantity $\Delta\nu(T_L/T_C)/(mK(m))$. Calculated results are compared with the observations of Davies (1971) for 110α, 138β, 158γ and 173δ in Fig. 16, and with the observations of Churchwell & Mezger (1970) for 109α, 137β, 157γ and 172δ in Fig. 17.

## 9.5 *Density distribution*

We compare the density distributions for Orion obtained by different methods.

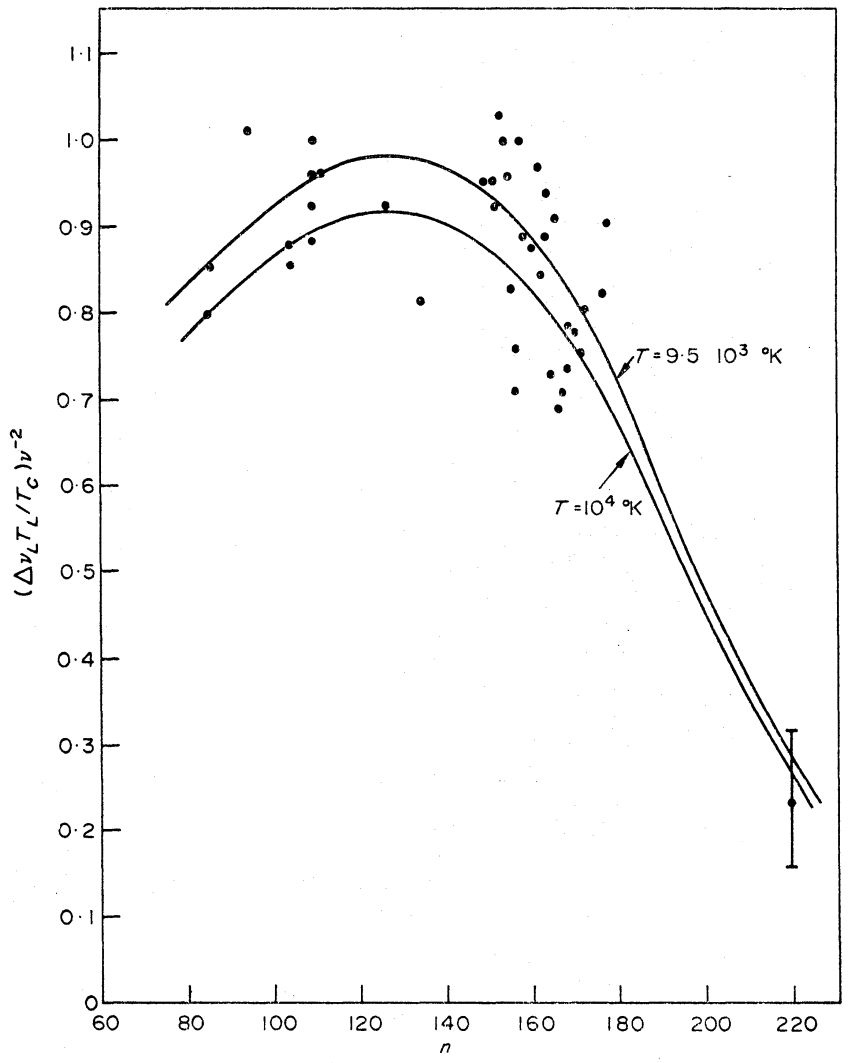


FIG. 15. *Values of* $\nu^{-2}(\Delta\nu T_L/T_C)$ *for* $n\alpha$ *lines in Orion, with* $\nu$ *in GHz and* $\Delta\nu$ *in kHz. Calculated curves are for the model of Table III and* $T = 10^{4\cdot0}K$ *and* $9{\cdot}5 \times 10^{3\cdot0}K$.

(i) *Photographs.* Osterbrock & Flather (1959) reproduce two Orion photographs taken with the 48-inch Schmidt telescope. A short exposure shows only the bright inner regions while a longer exposure shows much more extensive faint outer regions. Osterbrock and Flather take the outer radius of Orion to be 24′.

Hjellming & Davies (1970) reproduce a short exposure photograph taken with the 200-inch Mount Palomar telescope in conditions of excellent seeing. This shows a bright central region, with radius about 0·5′, containing bright filaments having angular widths no larger than a few seconds of arc. Aller (1956) reproduces a photograph of much longer exposure, taken with the Lick Crossley reflector, which also shows very complicated filamentary structures.

(ii) *Radio brightness contours.* Schraml & Mezger (1969) have observed Orion at 15·4 GHz with $\phi_{\mathrm{HPBW}} = 2'$. The assumption of spherical symmetry is seen to be a better approximation at radio wavelengths than at optical wavelengths—this is doubtless a consequence of partial obscuration by dust in the optical region. Webster & Altenhoff (1970) have made an aperture synthesis study at 2·7 GHz which shows complicated structures; it is estimated that densities as large as $4{\cdot}8 \times 10^4$ cm$^{-3}$ occur in dense condensations.

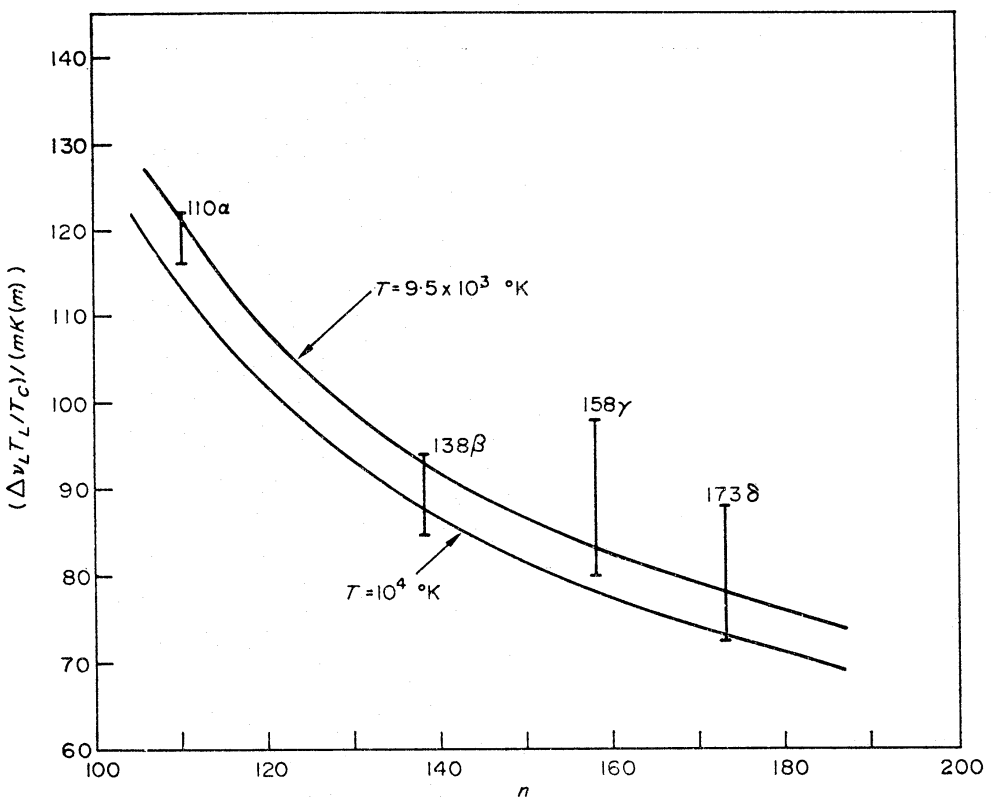


FIG. 16. *Values of* $\Delta\nu(T_L/T_C)/(mK(m))$, *with* $\Delta\nu$ *in kHz, for lines observed by Davies* (1971) *at frequencies close to 4·9 GHz. Calculated results are obtained using the model of Table III and* $T = 10^{4\circ}K$ *and* $9\cdot5 \times 10^{3\circ}K$.

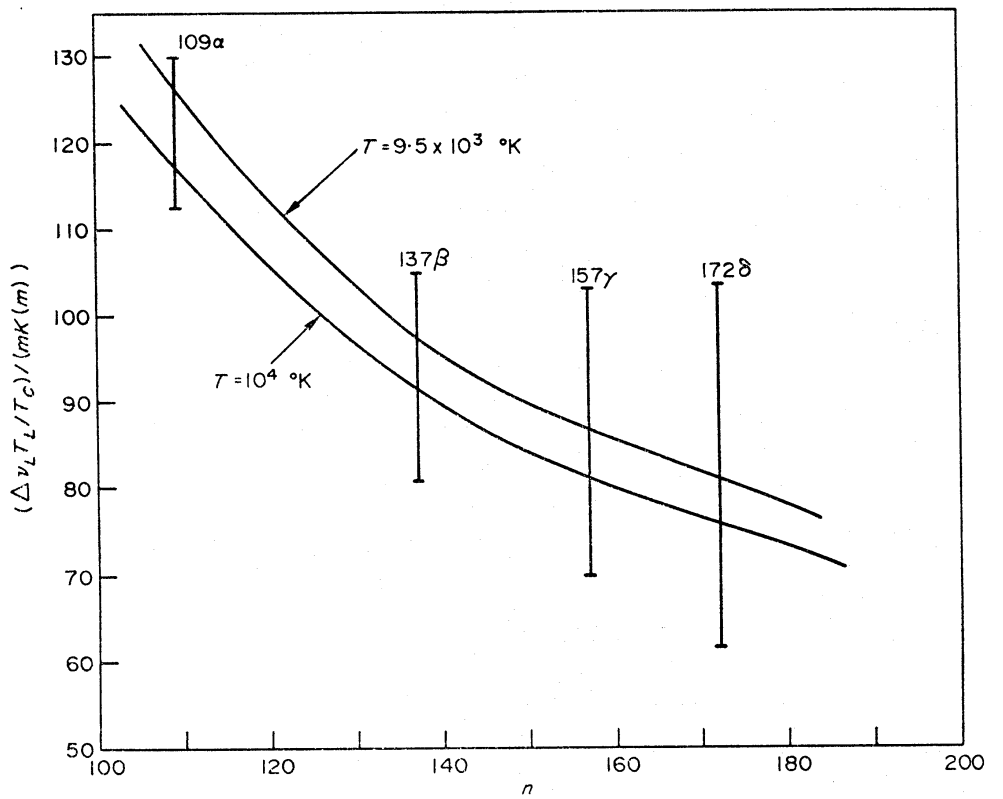


FIG. 17. *Values of* $\Delta\nu(T_L/T_C)/(mK(m))$ *for lines observed by Churchwell & Mezger* (1970) *at frequencies close to 5·0 GHz. Calculated results are obtained using the model of Table III and* $T = 10^{4\circ}K$ *and* $9\cdot5 \times 10^{3\circ}K$.

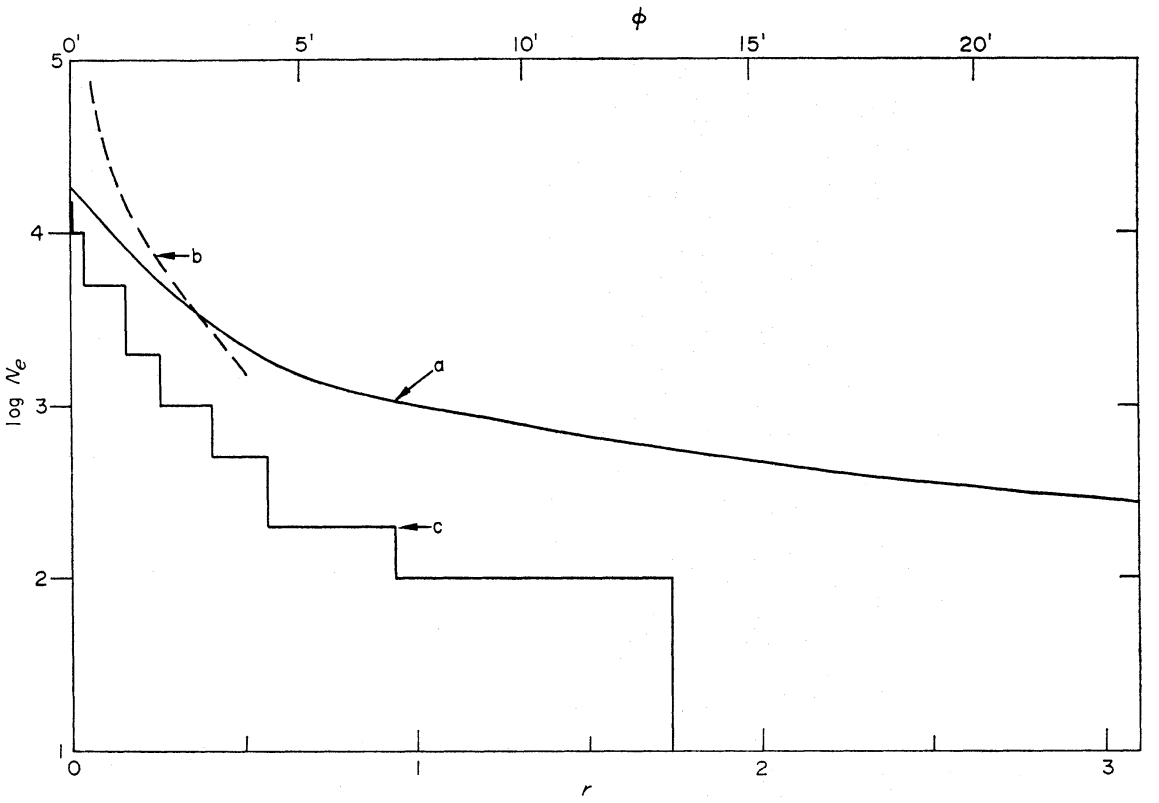


FIG. 18. *Values of log $N_e$ against r for three models of the Orion nebula ($N_e$ in cm$^{-3}$, r in psc): (a) the model of Osterbrock & Flather (1959) from [O II] observations; (b) the model of Danks & Meaburn (1971) from [S II] observations; (c) the model of the present paper.*

(iii) [*O* II] *and* [*S* II] *doublet ratios.* The ratios of the intensities of the components of the $^2D \rightarrow {}^4S$ doublets in [O II], and in [S II], are sensitive to $N_e$. In Fig. 18 our model is compared with models obtained by Osterbrock & Flather (1959) from [O II] observations and by Danks & Meaburn (1971) from [S II] observations. At densities above $10^4$ cm$^{-3}$ the [O II] ratios become insensitive to $N_e$ and the densities obtained from [S II] are therefore to be preferred.

(iv) *Discussion.* It was recognized by Osterbrock and Flather that their model could not be entirely correct, since it gives a total radio flux which is much too large, and that the explanation must be that local density fluctuations have not been taken into account. Let us suppose that the material is concentrated into clouds, with density $N_e = N_e^{(c)}$ inside the clouds and zero elsewhere. If it is further assumed that $N_e^{(c)}$ depends only on $r$, and that the fraction of space occupied by the clouds is independent of $r$, then the [O II] and [S II] models give values of $N_e^{(c)}(r)$.

From Fig. 18 it is seen that our model is not entirely correct, since it gives a total size which is too small; this is also a consequence of the neglect of local density fluctuations. However, our model and the [O II] and [S II] models give similar general trends for the variation of $N_e$ with $r$, and this leads us to believe that the basic theory used for the interpretation of the radio observations is correct, and that, when allowance is made for local density fluctuations, it should be possible to construct a model consistent with all radio and optical data.

9.6 *The electron temperature*

(i) *Optical observations.* At optical wavelengths the [O III] ratio

$$[I(\lambda\,4959)+I(\lambda\,5007)]/I(\lambda\,4363)$$

provides the best means of determining electron temperatures. Accurate measurements of this ratio have been made by Peimbert & Costero (1969) for three points in Orion. Table VII gives values of $T$ obtained from these measurements using the

TABLE VII

*Electron temperatures T deduced from the Orion [O III] intensity ratios of Peimbert & Costero (1969)*

| (a) | (b) | (c) | (d) | |
|---|---|---|---|---|
| Observed point | $\phi$ ′ | $T$ $10^3$°K | $N_e$ $10^4$ cm$^{-3}$ | $T$ $10^3$°K |
| I | 0·5 | 8·5 | 5·0 | 8·0 |
| II | 0·5 | 9·0 | 5·0 | 8·5 |
| III | 3·0 | 9·0 | 0·3 | 9·0 |

(a) The positions of the observed points are given by Peimbert & Costero (1969).
(b) Distance from centre in seconds of arc.
(c) $T$ calculated neglecting collisional de-excitation.
(d) $T$ calculated allowing for collisional de-excitation, and values of $N_e$ assumed.

collision strengths of Eissner *et al.* (1969). Two cases are considered: (a) $T$ is calculated neglecting collisional de-excitation; (b) $T$ is calculated assuming values of $N_e$ and allowing for collisional de-excitation. These results indicate that $T$ is in the range $8\times10^3$ to $9\times10^3$°K.

(ii) *Radio observations.* The results of our calculations using the model of Table III show that the agreement with observations is better for $T = 9{\cdot}5\times10^3$ than for $T = 1\times10^4$°K (Figs 15, 16 and 17). It should be noted, however, that the only observations which are sensitive to $T$ and insensitive to the structure of the model are the line-to-continuum ratios for the high-order lines observed at higher frequencies. The accuracy of these observations is not such as to allow a precise determination of $T$ to be made.

We may conclude that, to within the accuracy of the observations and of the calculated collision strengths, the temperatures determined from radio and optical data are in agreement.

ACKNOWLEDGMENTS

This work has been supported by the Science Research Council, and by the award of an IBM Fellowship to M. Brocklehurst.

We wish to express our thanks to Dr G. Rybicki for supplying the subroutine used for the calculation of Voigt functions, to thank Drs R. D. Davies, A. Pedlar, E. Churchwell and D. G. Hummer for helpful discussions and to thank Mr T. Venis for tracing the diagrams.

*Department of Physics, University College London*

## REFERENCES


Aller, L. H., 1956. *Gaseous Nebulae*, Chapman and Hall, London, Fig. II : 2.

Ball, J. A., Cesarsky, D., Dupree, A. K., Goldberg, L. & Lilley, A. E., 1970. *Astrophys. J. Lett.*, **162**, L25.

Brocklehurst, M., 1970. *Mon. Not. R. astr. Soc.*, **148**, 417.

Brocklehurst, M., 1971. *Mon. Not. R. astr. Soc.*, **153**, 471.

Brocklehurst, M. & Leeman, S., 1971. *Astrophys. Lett.*, **9**, 35.

Brocklehurst, M. & Seaton, M. J., 1971. *Astrophys. Lett.*, **9**, 139.

Churchwell, E., 1971. *Astr. Astrophys.*, **15**, 90.

Churchwell, E. & Mezger, P. G., 1970. *Astrophys. Lett.*, **5**, 227.

Danks, A. C. & Meaburn, J., 1971. *Astrophys. & Space Sci.*, **11**, 398.

Davies, R. D., 1971. *Astrophys. J.*, **163**, 479.

Dyson, J. E., 1969. *Astrophys. J.*, **155**, 4.

Eissner, W., Martins, P. de A. P., Nussbaumer, H., Saraph, H. E. & Seaton, M. J., 1969. *Mon. Not. R. astr. Soc.*, **146**, 63.

Goldberg, L., 1966. *Astrophys. J.*, **144**, 1225.

Gordon, M. A., 1970. *Astrophys. Lett.*, **6**, 27.

Griem, H., 1967. *Astrophys. J.*, **148**, 547.

Hjellming, R. M. & Churchwell, E., 1969. *Astrophys. Lett.*, **4**, 165.

Hjellming, R. M. & Davies, R. D., 1970. *Astr. Astrophys.*, **5**, 53.

Hjellming, R. M. & Gordon, M. A., 1971. *Astrophys. J.*, **164**, 47.

Hjellming, R. M., Andrews, M. H. & Sejnowski, T. J., 1969. *Astrophys. J.*, **157**, 573.

Kardashev, N. S., 1959. *Soviet Astr.—A.J.*, **3**, 813.

Menzel, D. H., 1968. *Nature*, **218**, 756.

Oster, L., 1961. *Rev. mod. Phys.*, **33**, 525.

Osterbrock, D. E. & Flather, E., 1959. *Astrophys. J.*, **129**, 26.

Peach, G., 1972. *Astrophys. Lett.*, **10**, 129.

Pedlar, A., 1971. Ph.D. Thesis. Univ. of Manchester.

Pedlar, A. & Davies, R. D., 1971. *Nature, Phys. Science*, **231**, 49.

Peimbert, M. & Costero, R., 1969. *Bol. Obs. Tonantzintla Tombaya*, **5**, 3.

Percival, I. C. & Richards, D., 1969. *Astrophys. Lett.*, **4**, 235. (See also, 1970. *J. Phys. B. Atom. Molec.*, **3**, 316.)

Schraml, J. & Mezger, P. G., 1969. *Astrophys. J.*, **156**, 269.

Seaton, M. J., 1971. *Highlights of Astronomy*, Vol. 2, p. 288, ed. C. de Jager, Reidel, Dordrecht-Holland.

Simpson, J. P., 1970. Thesis, Univ. of Calif., Berkeley.

Webster, W. J. & Altenhoff, W. J., 1970. *Astrophys. Lett.*, **5**, 233.